

Surrogate-Assisted Targeted Learning for Delayed Outcomes under Administrative Censoring

Lin Li*

March 2026

Abstract

Delayed primary outcomes and administratively censored follow-up create a general semiparametric estimation problem: the target causal functional depends on an endpoint observed only for a shrinking subset of units at analysis time, while earlier surrogate measurements remain widely available. In such settings, inverse-probability-weighted estimators can become unstable as observation probabilities approach the positivity boundary, and complete-case model-based analyses can be highly sensitive to outcome-model specification.

We develop a surrogate-assisted targeted minimum loss estimator for this nested causal functional. Identification proceeds through a surrogate-bridge representation that integrates an observed-outcome regression over the conditional surrogate distribution, thereby avoiding inverse observation weights in the target parameter itself. We show that the estimator is asymptotically linear and doubly robust (in the sense that first-order bias vanishes when either nuisance component is consistently estimated), and we characterize two structural features of the problem: under surrogate-mediated missing at random, the censoring mechanism contributes no separate tangent-space component to the efficient influence function; and for nested bridge functionals, a one-step debiased machine-learning construction leaves a second-order cross-product remainder involving the conditional surrogate law. The proposed two-stage targeting step removes this term without requiring direct estimation of that law.

Simulation studies demonstrate stable finite-sample performance under substantial administrative censoring, and a design-calibrated analysis based on the Washington State EPT study illustrates the method in a realistic stepped-wedge cluster-randomized setting.

*Department of Biostatistics, University of California San Diego.

1 Introduction

Many modern studies measure the primary endpoint only after substantial delay, while shorter-term surrogate outcomes are available much earlier in follow-up. When analysis occurs before all primary outcomes mature, the resulting observed-data structure poses a distinctive semiparametric problem: the estimand depends on a delayed endpoint observed only for a subset of units whose observation probability may approach the positivity boundary, yet a surrogate remains broadly observed across the design space. In such settings, estimators that rely directly on inverse observation weights can become unstable as observation probabilities become small, whereas complete-case model-based analyses may inherit strong sensitivity to outcome-model specification.

This paper studies that problem through a surrogate-bridge formulation for causal effect estimation under administrative censoring. The key idea is to identify the target functional — the average treatment effect $\Psi(P_0) = \mathbb{E}[Y(1) - Y(0)]$ — by integrating an observed-outcome regression over the conditional surrogate law, rather than by placing the inverse observation probability directly in the target parameter. This perspective leads naturally to a targeted learning estimator and exposes new structure in the corresponding semiparametric theory.

A stepped-wedge cluster randomized trial (SW-CRT) provides a particularly sharp motivating example. Because treatment rollout is tied to calendar time, late-crossing clusters may have little opportunity to realize the delayed endpoint before study closure. But the underlying statistical issue is broader than stepped-wedge designs: whenever an early surrogate is observed widely and a primary endpoint is administratively censored at analysis time, the analyst faces the same nested surrogate-bridge problem. We therefore use the stepped-wedge setting as a concrete and practically important instance of a more general semiparametric estimation problem.

Limitations of standard approaches. Parametric mixed models [Hussey and Hughes, 2007, Hemming and Taljaard, 2020, Hughes et al., 2020] restrict attention to the complete-case sub-cohort $\{\Delta_{ijt} = 1\}$ and require correct specification of both the secular time trend and the missing-data mechanism. IPCW estimators [Robins et al., 1994, Bang and Robins, 2005] place g_{Δ}^{-1} directly in the estimating equation; even moderate concentration of g_{Δ} near zero for late-crossing clusters produces severe variance inflation, and in the near-boundary regime these estimators may fail to admit regular asymptotic approximations.

Contributions. This paper makes three methodological contributions.

First, we identify a class of causal functionals under surrogate-mediated administrative censoring through a nested bridge representation (Theorem 1) that avoids inverse observation weights in the target parameter. The surrogate-bridge G-computation formula identifies $\Psi(P_0)$ via nested conditional expectations over the observed surrogate distribution, replacing the unstable g_{Δ}^{-1} with a support positivity condition on the complete-case outcome regression.

Second, we characterize the efficient-score structure of this problem (Section 3): under surrogate-mediated missing at random, the censoring mechanism contributes no separate tangent-space component to the efficient influence function (Lemma 1), so estimating g_{Δ} does not reduce the efficiency bound; and under clustered dependence, valid inference requires aggregation of influence contributions at the cluster level rather than averaging (Lemma 2).

Third, we show that for this nested functional, a standard one-step debiased machine-learning construction generally leaves a second-order cross-product remainder R_{SY} involving the conditional surrogate law f_S (Proposition 2); the proposed two-stage targeted minimum loss procedure removes that term without requiring direct estimation of f_S , achieving \sqrt{J} -consistency under a product-rate condition on the remaining nuisance estimators (Theorem 2).

Related statistical work. Our work sits at the intersection of semiparametric missing-data theory, targeted learning, and modern debiased machine learning. Classical AIPW theory [Robins et al., 1994, Bickel et al., 1993] characterizes efficient estimation with missing outcomes via tangent space decomposition, but does not address the nested bridge structure considered here. Existing SW-CRT methodology [Hussey and Hughes, 2007, Hemming and Taljaard, 2020, Kasza et al., 2019, Hughes et al., 2020] largely remains centered on parametric mixed models and does not accommodate the present surrogate-assisted functional. The surrogate outcome literature [Gilbert et al., 2008, Frangakis and Rubin, 2002] addresses a complementary problem — evaluating treatment effects when the primary outcome is *rare*, not delayed — and their identification strategies do not extend to the near-boundary censoring regime. Luedtke et al. [2017] construct the closest prior estimator: a semiparametric surrogate-index estimator for i.i.d. data whose identification formula is structurally related to ours. However, their asymptotic linearity argument requires a uniform positivity lower bound on g_{Δ} , which the SW-CRT’s calendar-driven censoring structure violates for late-crossing clusters; the present surrogate-bridge approach does not place g_{Δ}^{-1} in the target parameter and therefore does not require this condition. Cluster-level targeted learning [Balzer et al., 2016, 2021] establishes the importance of clusterwise influence aggregation for valid sandwich inference in group-randomized trials, but without the bridge-based identifica-

tion and nested targeting problem studied here. The debiased machine learning framework [Chernozhukov et al., 2018] provides general product-rate guarantees via sample splitting, yet in the present setting a one-step construction leaves a nested cross-product remainder R_{SY} involving the conditional surrogate law f_S that cross-fitting does not eliminate. The contribution of this paper is to isolate that remainder explicitly (Proposition 2) and show how a second targeting step absorbs it without estimating f_S .¹

Section 2 defines the observed data structure and establishes non-parametric identification via the surrogate-bridge representation. Section 3 develops the semiparametric theory: the EIC decomposition, the vanishing censoring-mechanism component (Lemma 1), the cluster-level summation rule (Lemma 2), and the nested cross-product remainder that makes two-stage targeting necessary (Proposition 2). Section 4 constructs the SA-TMLE as the direct solution to the theoretical constraints identified in Section 3. Section 5 establishes asymptotic linearity, double robustness, and the Berry–Esseen finite-sample coverage bound. Section 6 reports Monte Carlo experiments across three scenario blocks. Section 7 provides a brief design-calibrated illustration using the Washington State EPT trial.

Although our motivating application is a stepped-wedge cluster trial, the framework is not tied to that design. The same statistical structure arises whenever a delayed primary outcome is observed only for a subset of units at analysis time, an earlier surrogate is broadly available, and identification proceeds through a nested bridge representation. The paper is best understood not as a stepped-wedge method but as a general semiparametric framework for nested surrogate-bridge inference under administrative censoring, with stepped-wedge trials providing a particularly consequential use case.

2 Data Structure and Identification

We first describe the observed-data structure and identification strategy in the stepped-wedge cluster-randomized setting, which serves as our running example of a broader class of surrogate-assisted problems with administratively censored delayed outcomes.

Consider a SW-CRT with J clusters, T calendar time steps, and n_j individuals in cluster j ($N = \sum_j n_j$ total). Each cluster crosses over once at a design-determined time $\tau_j \in \{2, \dots, T\}$, so $A_{jt} = I(t \geq \tau_j)$; crossover times are assigned uniformly at random and

¹See Kennedy [2022] for a comprehensive review of debiased machine learning. Proposition 2 gives the formal derivation.

Table 1: When to use each estimator: a practical comparison for stepped-wedge trials with delayed outcomes.

	GLMM	IPCW/AIPW	SA-TMLE (proposed)
Target parameter	Conditional treatment effect (model-based)	Population ATE	Population ATE
Key assumptions	Correct outcome model specification (secular trend, random effects)	Observation positivity: g_{Δ}^{-1} must be well-behaved	Support positivity for $E[Y S, A, W, t]$; surrogate-mediated MAR
Handles heavy censoring?	No: complete-case analysis drops late-crossing clusters entirely	Poorly: variance inflates as $g_{\Delta} \rightarrow 0$	Yes: bypasses g_{Δ}^{-1} via surrogate bridge
Requires surrogate?	No	No	Yes
Double robustness?	No	Yes (but requires bounded g_{Δ}^{-1})	Yes (asymptotically; finite-sample behavior may be asymmetric under nuisance misspecification)
Nonparametric nuisance?	No (parametric outcome model)	Yes (machine learning compatible)	Yes (machine learning compatible)
Best suited for	Low censoring, well-understood secular trends, no surrogate available	Moderate censoring with good observation-positivity overlap	Substantial administrative censoring with an available early surrogate

$A_{j1} = 0$ for all j . The observed data tuple is

$$O_{ijt} = (W_{ijt}, A_{jt}, S_{ijt}, \Delta_{ijt}, \Delta_{ijt} \cdot Y_{ijt}) \sim P_0, \quad (1)$$

where $W_{ijt} \in \mathbb{R}^p$ are baseline covariates; S_{ijt} is the short-term surrogate; $\Delta_{ijt} \in \{0, 1\}$ indicates whether the delayed primary outcome was observed by the administrative end date; and Y_{ijt} is that outcome. The product $\Delta_{ijt} \cdot Y_{ijt}$ makes explicit that Y is structurally missing for late-crossing clusters.

Let $\mathbf{U} = (U_W, U_A, b_j, U_S, U_\Delta, U_Y)$ denote the exogenous noise variables. The cluster-level random effect $b_j \stackrel{\text{i.i.d.}}{\sim} \mathcal{N}(0, \sigma_b^2)$ is i.i.d. across clusters. All other components are individual-level noise terms assumed mutually independent across individuals and clusters.

The following system defines the endogenous variables in their causal time-ordering:

$$W_{ijt} = f_W(U_{W,ij}), \quad (\text{baseline covariates}) \quad (2)$$

$$A_{jt} = I(t \geq \tau_j), \quad \tau_j = f_A(U_{A,j}), \quad (\text{treatment; deterministic given } \tau_j) \quad (3)$$

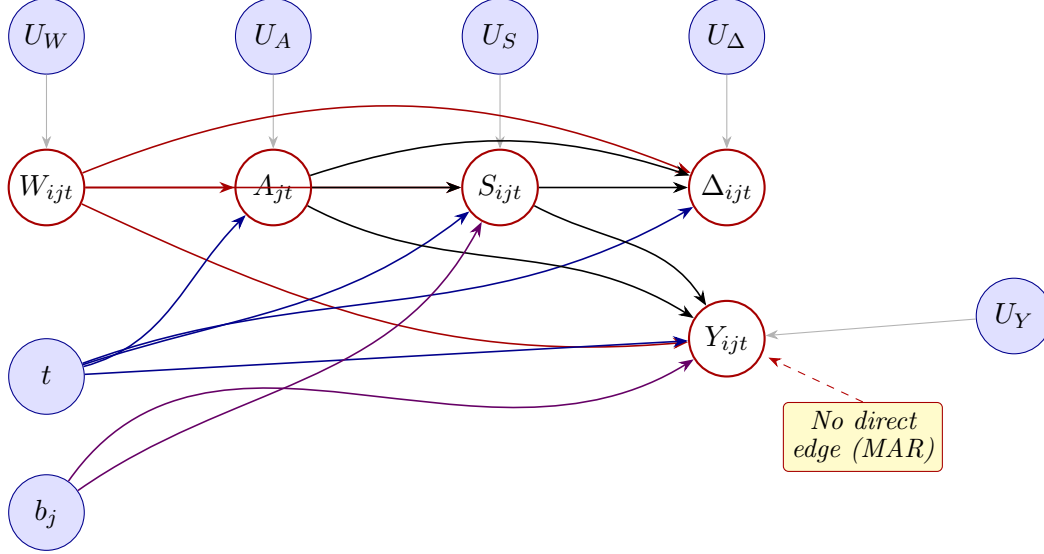
$$S_{ijt} = f_S(W_{ijt}, A_{jt}, b_j, t, U_{S,ijt}), \quad (\text{short-term surrogate}) \quad (4)$$

$$\Delta_{ijt} = f_\Delta(S_{ijt}, A_{jt}, W_{ijt}, t, U_{\Delta,ijt}), \quad (\text{observation indicator}) \quad (5)$$

$$Y_{ijt} = f_Y(W_{ijt}, A_{jt}, S_{ijt}, b_j, t, U_{Y,ijt}). \quad (\text{delayed primary outcome}) \quad (6)$$

Three structural features deserve emphasis. First, A_{jt} is deterministic given τ_j ; the treatment mechanism is *known by design* and does not require data-adaptive estimation (see Remark 4). Second, the cluster random effect b_j enters both f_S and f_Y , inducing the ICC among all observations within cluster j (Remark 1). Third — and most critically — Y does not appear in f_Δ and U_Δ does not appear in f_Y . This is the structural encoding of Assumption 3: conditional on S , the censoring indicator Δ is independent of the outcome Y . In DAG terms, there is no directed edge $Y_{ijt} \rightarrow \Delta_{ijt}$ (Figure 1).

Remark 1 (Intra-cluster correlation). *The shared cluster random effect $b_j \stackrel{\text{i.i.d.}}{\sim} \mathcal{N}(0, \sigma_b^2)$ enters both f_S and f_Y , inducing $\text{ICC} = \sigma_b^2 / (\sigma_b^2 + \sigma_\epsilon^2)$ among individuals within a cluster. The two methodological consequences are: (i) inference must use the cluster-robust sandwich estimator of Section 3; and (ii) Super Learner cross-validation must be performed at the cluster level (Supplement, Section S3). The TMLE estimator itself makes no parametric assumption about b_j ; the Gaussian model governs the simulation DGP only.*



Time ordering: $W \rightarrow A \rightarrow S \rightarrow \Delta \rightarrow Y$

Figure 1: Directed Acyclic Graph for the SW-CRT Structural Causal Model. *Red* circles: endogenous variables. *Blue* circles: exogenous and design variables. *Violet* arrows: cluster random effect b_j , the source of ICC. The critical structural feature is the **absence** of a directed edge $Y_{ijt} \rightarrow \Delta_{ijt}$, encoding Assumption 3: once S_{ijt} is observed, the censoring probability depends on S but not directly on the unobserved Y . The secular time trend t acts as a common cause of all endogenous variables and must be adjusted for in estimation.

2.1 Potential Outcomes and the Causal Target

For intervention value $a \in \{0, 1\}$, let $S_{ijt}(a)$ and $Y_{ijt}(a)$ denote the potential outcomes obtained by the intervention $\text{do}(A_{ijt} = a)$ in the SCM. The causal Average Treatment Effect (ATE) is:

$$\Psi(P_0) = \mathbb{E}[Y_{ijt}(1) - Y_{ijt}(0)], \quad (7)$$

where the expectation is over the marginal distribution of (W_{ijt}, b_j, t) in the trial. The identification of $\Psi(P_0)$ from P_0 is the subject of Section 2.2.

2.2 Non-Parametric Identification

The central identification insight is that the target causal effect can be represented through a surrogate bridge: one first learns the observed-outcome regression among units with realized primary outcomes and then integrates that regression over the treatment-specific surrogate distribution. This representation identifies the causal estimand without placing inverse observation weights in the target functional itself, which is precisely what makes it attractive in regimes where observation probabilities become small.

We establish the following assumptions to formalize this representation.

Assumption 1 (Consistency). *For any observed treatment assignment $A_{jt} = a$, $S_{ijt} = S_{ijt}(a)$ and $Y_{ijt} = Y_{ijt}(a)$.*

Assumption 2 (Sequential Randomization). *Conditional on the cluster history, treatment is independent of potential outcomes:*

$$(Y(0), Y(1), S(0), S(1)) \perp A_{jt} \mid W_{ijt}, t. \quad (8)$$

This holds by design: $A_{jt} = I(t \geq \tau_j)$ and τ_j is randomized independently of individual outcomes.

Assumption 3 (Surrogate-Mediated Missing at Random). *The unobserved outcome provides no additional information about the censoring probability once the surrogate is known [Rubin, 1976]:*

$$P(\Delta_{ijt} = 1 \mid Y_{ijt}, S_{ijt}, A_{jt}, W_{ijt}, t) = P(\Delta_{ijt} = 1 \mid S_{ijt}, A_{jt}, W_{ijt}, t). \quad (9)$$

This is structurally encoded in the SCM by the absence of the edge $Y_{ijt} \rightarrow \Delta_{ijt}$ (Figure 1, Equation (5)).

Remark 2 (Practical plausibility of Assumption 3). *Assumption 3 is most defensible when missingness is administrative (calendar-driven) rather than informative (health-driven). In the SW-CRT setting, the dominant censoring mechanism — the trial’s fixed end date — is independent of Y_{ijt} conditional on S_{ijt} . A strong surrogate candidate satisfies three properties: (i) causal proximity: S lies on or near the pathway $A \rightarrow S \rightarrow Y$; (ii) temporal availability: S is observed for all individuals regardless of crossover time; and (iii) biological stationarity: $\mathbb{E}[Y \mid S, A, W, t]$ does not change systematically over calendar time. Examples include 3-month viral load predicting 12-month suppression in HIV trials, and discharge-process scores predicting 30-day readmission in quality-improvement SW-CRTs.*

Assumption 4 (Support Positivity for the Observed Outcome Regression). *There exists a constant $c > 0$ such that, for all (s, a, w, t) in the support of (S, A, W, t) relevant to the target parameter,*

$$P(\Delta_{ijt} = 1 \mid S_{ijt} = s, A_{jt} = a, W_{ijt} = w, t) \geq c. \quad (10)$$

Remark 3 (Support positivity versus inverse-weighting regularity). *Assumption 4 is a support condition for identifying $E[Y \mid S, A, W, t]$ from the observed cohort $\{\Delta = 1\}$, not an inverse-weighting regularity condition. IPCW-type estimators are sensitive to small values*

of g_Δ because g_Δ^{-1} appears directly in the influence function, so that even when Assumption 4 holds with a small constant c , the IPCW estimating equation becomes highly variable. The surrogate-bridge parameter, by contrast, does not contain g_Δ^{-1} in the target functional; it requires only that the complete-case outcome regression $E[Y \mid S, A, W, t, \Delta = 1]$ be well-defined on the support over which the surrogate-bridge formula integrates.

Assumption 5 (Design-Based Treatment Support). *The marginal treatment probability, averaged over the trial design space, is non-degenerate:*

$$0 < \mathbb{E}_t[g_A(1 \mid W, t)] < 1. \quad (11)$$

Remark 4 (Why Treatment Positivity Holds Marginally Despite Pointwise Violations). *At any fixed time t and cluster j , the treatment assignment is deterministic: $A_{jt} = I(t \geq \tau_j)$, so pointwise positivity $0 < P(A_{jt} = 1 \mid W, t) < 1$ fails everywhere. A naive reading would therefore conclude that treatment positivity is structurally violated by the SW-CRT design.*

*This is resolved by observing that the identification formula (13) marginalizes over the trial's design space, averaging jointly over both W and t . The design-based propensity is **known by construction** from the randomization schedule. Under a uniform randomization of crossover times:*

$$g_A(1 \mid W, t) = P(\tau_j \leq t) = \frac{t-1}{T-1}. \quad (12)$$

Averaging over the interior steps $t \in \{2, \dots, T-1\}$ yields $\mathbb{E}_t[g_A(1 \mid W, t)] = 1/2$, so Assumption 5 holds. In practice, boundary steps $t = 1$ and $t = T$ should be excluded, as g_A equals 0 and 1 respectively at these endpoints.

A further consequence is that g_A need not be estimated from the data. In Section 4, we plug in the design-based propensity directly, eliminating one source of nuisance estimation error from the second-order remainder R_2 (Supplement, Section S2).

Theorem 1 (Identification via a Surrogate Bridge under Support Positivity). *Under Assumptions 1–5, the causal ATE is identified by the longitudinal G-computation formula:*

$$\begin{aligned} \Psi(P_0) = & \mathbb{E}_{W,t} \left(\mathbb{E}_{S|A=1,W,t} [\mathbb{E}[Y \mid S, A = 1, W, t, \Delta = 1]] \right. \\ & \left. - \mathbb{E}_{S|A=0,W,t} [\mathbb{E}[Y \mid S, A = 0, W, t, \Delta = 1]] \right). \end{aligned} \quad (13)$$

Proof. By Assumptions 1 (Consistency) and 2 (Sequential Randomization), the potential

outcome mean satisfies:

$$\mathbb{E}[Y(a) \mid S(a), W, t] = \mathbb{E}[Y \mid S, A = a, W, t]. \quad (14)$$

By Assumption 3 (Surrogate-Mediated MAR) and Assumption 4 (Support Positivity), we may condition on the observed cohort ($\Delta = 1$):

$$\mathbb{E}[Y \mid S, A = a, W, t] = \mathbb{E}[Y \mid S, A = a, W, t, \Delta = 1] \equiv \bar{Q}_Y(S, a, W, t). \quad (15)$$

Integrating \bar{Q}_Y over the conditional surrogate distribution:

$$\mathbb{E}[Y(a) \mid W = w, t] = \int \bar{Q}_Y(s, a, w, t) dP(s \mid a, w, t) \equiv \bar{Q}_{\text{int}}(a, w, t). \quad (16)$$

Marginalizing over the trial design space yields (13). □ □

3 Semiparametric Theory

We now study the surrogate-bridge estimand as a semiparametric functional. This perspective is central for two reasons. First, it reveals the efficient-score geometry induced by surrogate-mediated censoring and clustered dependence: the censoring mechanism contributes no separate tangent-space component, and the cluster structure requires summation rather than averaging of influence contributions. Second, it clarifies why a standard one-step debiased estimator is not sufficient for the nested bridge problem: the second-order remainder contains a cross-product term involving the conditional surrogate law that is not removed by ordinary cross-fitting. The resulting analysis motivates the specific two-stage targeting construction developed in Section 4.

3.1 EIC Decomposition

The individual-level EIC components, whose derivation is provided in Supplement, Section S2, are as follows. For treatment $a \in \{0, 1\}$:

$$D_{Y,a}(O_{ijt}) = \frac{I(A = a) \Delta}{g_A(a \mid W, t) g_\Delta(1 \mid S, A, W, t)} (Y - \bar{Q}_Y(S, a, W, t)), \quad (17)$$

$$D_{S,a}(O_{ijt}) = \frac{I(A = a)}{g_A(a \mid W, t)} (\bar{Q}_Y(S, a, W, t) - \bar{Q}_{\text{int}}(a, W, t)), \quad (18)$$

$$D_{W,a}(O_{ijt}) = \bar{Q}_{\text{int}}(a, W, t) - \hat{\Psi}_a, \quad (19)$$

where $\hat{\Psi}_a = N^{-1} \sum_{j,i} \bar{Q}_{\text{int}}^*(a, W_{ijt}, t_{ij})$.

In Equation (18), both nuisance functions are evaluated at the fixed intervention value a rather than the observed random variable A . Under the indicator $I(A = a)$, the two are numerically equal on the support of the data, but the fixed-argument form is essential: it makes explicit that $\bar{Q}_Y(S, a, W, t)$ and $\bar{Q}_{\text{int}}(a, W, t)$ are counterfactual predictions under $\text{do}(A = a)$, consistent with the identification formula (13). Writing A in the argument of $D_{S,a}$ would obscure this causal interpretation and introduce an inconsistency with the identification strategy.

The total individual EIC is:

$$D^*(O_{ijt}) = (D_{Y,1} + D_{S,1} + D_{W,1}) - (D_{Y,0} + D_{S,0} + D_{W,0}). \quad (20)$$

The first structural result shows that surrogate-mediated censoring changes the identification strategy but not the efficient-score geometry in the usual missingness direction: once the surrogate is conditioned upon, the censoring mechanism contributes no separate tangent-space component.

Lemma 1 (Vanishing \mathcal{T}_Δ Component). *Under Assumption 3 (Surrogate-Mediated MAR), the pathwise derivative of Ψ_a in the \mathcal{T}_Δ direction is identically zero: the EIC has no censoring-mechanism component.*

Proof. Consider a parametric submodel perturbing only g_Δ along score $h_\Delta \in \mathcal{T}_\Delta$. The identification formula (Equation (13)) reaches g_Δ only through the restriction of $\mathbb{E}[Y | S, A=a, W, t]$ to $\{\Delta = 1\}$. By Assumption 3, $P(\Delta = 1 | Y, S, A, W, t) = P(\Delta = 1 | S, A, W, t)$, so perturbing g_Δ while holding $\bar{Q}_Y(S, a, W, t)$ and $P(S | a, W, t)$ fixed leaves $\bar{Q}_{\text{int}}(a, W, t)$ unchanged. Consequently,

$$\frac{d}{d\epsilon} \Psi_a(P_\epsilon) \Big|_{\epsilon=0} = \mathbb{E}_P[(\bar{Q}_{\text{int}}(a, W, t) - \Psi_a) h_\Delta(O)] = 0, \quad (21)$$

where the final equality holds because $\bar{Q}_{\text{int}}(a, W, t) - \Psi_a$ is P -mean-zero and orthogonal to any score supported only on variations in the censoring mechanism. Without Assumption 3, the censoring direction contributes a non-zero term involving the unidentified quantity $\mathbb{E}[Y | S, A, W, t, \Delta = 0]$, rendering the EIC non-estimable from observed data. \square \square

The second structural result concerns the correct level of influence aggregation. Because the estimand is defined through cluster-randomized data with arbitrary within-cluster dependence, the efficient contribution of a cluster is obtained by summation rather than averaging

of individual terms; this is essential for valid semiparametric variance estimation under unequal cluster sizes.

Lemma 2 (Cluster-Level Summation Rule). *Let $O_j = \{O_{ijt} : i = 1, \dots, n_j, t = 1, \dots, T\}$ denote the full data vector for cluster j , and let Ψ be expressed as a functional of the cluster-level distribution P_j . The Riesz representer of the pathwise derivative in $L^2(P_j)$ — equivalently, the cluster-level EIC — is the sum (not average) of individual EICs:*

$$\text{EIC}_j = \sum_{i=1}^{n_j} \sum_{t=1}^T D^*(O_{ijt}). \quad (22)$$

Averaging by $n_j T$ would rescale the influence curve, rendering the sandwich variance estimator inconsistent under unbalanced cluster sizes and non-negligible ICC.

Proof. Collecting Proposition 3.1 for $a = 1$ minus $a = 0$:

$$D^*(O_{ijt}) = (D_{Y,1} + D_{S,1} + D_{W,1}) - (D_{Y,0} + D_{S,0} + D_{W,0}). \quad (23)$$

Because clusters are the i.i.d. units of randomization, the parameter Ψ is a functional of the cluster-level distribution P_j of $O_j = \{O_{ijt} : i = 1, \dots, n_j, t = 1, \dots, T\}$:

$$\Psi = \frac{1}{N} \sum_{j=1}^J \sum_{i=1}^{n_j} [\bar{Q}_{\text{int}}(1, W_{ij}, t_{ij}) - \bar{Q}_{\text{int}}(0, W_{ij}, t_{ij})]. \quad (24)$$

Applying the pathwise derivative to a submodel $P_{j,\epsilon}$ perturbing only cluster j along score $h_j(O_j)$, the chain rule over the additive structure gives

$$\frac{d}{d\epsilon} \Psi(P_{j,\epsilon})|_{\epsilon=0} = \mathbb{E}_{P_j} \left[\left(\sum_{i=1}^{n_j} \sum_{t=1}^T D^*(O_{ijt}) \right) h_j(O_j) \right]. \quad (25)$$

The Riesz representer in $L^2(P_j)$ is therefore the *sum* (not average) of individual EICs:

$$\text{EIC}_j = \sum_{i=1}^{n_j} \sum_{t=1}^T D^*(O_{ijt}). \quad (26)$$

Summation absorbs both the intra-cluster correlation (ICC) across individuals at a given step and the serial correlation across steps induced by the secular trend; averaging by n_j would rescale the influence curve and produce inconsistent variance estimates under unbalanced cluster sizes. \square

3.2 The Nested Cross-Product Remainder and the Necessity of Two-Stage Targeting

The previous two lemmas establish the efficient-score structure of the surrogate-bridge functional — the core semiparametric object of this paper — but they do not yet determine the appropriate estimator. A natural question is whether a standard one-step debiased machine-learning construction suffices. The next result shows that, for nested bridge functionals, the answer is generally no. Even after cross-fitting removes first-order empirical-process terms, a second-order cross-product remainder R_{SY} remains because the bridge functional depends jointly on the outcome regression and the conditional surrogate law f_S . This remainder is not a fluctuation term and therefore is not eliminated by ordinary sample splitting. This is the semiparametric obstruction that the two-stage targeting step of Section 4 is specifically designed to resolve.

Proposition 1 (Nested Cross-Product Term in the DML Remainder). *Let $f_S(\cdot | a, W, t) \equiv P_0(S \in \cdot | A = a, W, t)$ denote the conditional density of the surrogate, and let \hat{f}_S be any estimator of f_S independent of the SA-TMLE nuisance estimators. Define the plug-in integral estimator $\hat{Q}_{\text{int}}^{\text{DML}}(a, W, t) \equiv \int \hat{Q}(s, a, W, t) \hat{f}_S(s | a, W, t) d\mu(s)$, which constructs \bar{Q}_{int} as an integral of \hat{Q} against \hat{f}_S .*

For the DML one-step estimator $\hat{\Psi}^{\text{DML}} = \hat{\Psi}_{\text{plug-in}}^{\text{DML}} + N^{-1} \sum_{j,i,t} D^(O_{ijt}; \hat{Q}, \hat{Q}_{\text{int}}^{\text{DML}}, \hat{g}_A, \hat{g}_\Delta)$ based on this construction, the von Mises expansion yields:*

$$\hat{\Psi}^{\text{DML}} - \Psi(P_0) = \frac{1}{J} \sum_{j=1}^J \text{EIC}_j + R_2^{\text{TMLE}}(\hat{P}, P_0) + R_{SY}(\hat{P}, P_0) + o_P(J^{-1/2}), \quad (27)$$

where R_2^{TMLE} is the TMLE remainder (Supplement, Section S2.4) and the nested cross-product remainder is

$$R_{SY}(\hat{P}, P_0) = \sum_{a \in \{0,1\}} (-1)^{1-a} \iint (\hat{Q} - \bar{Q}_Y^0)(s, a, w, t) (\hat{f}_S - f_S^0)(s | a, w, t) d\mu(s) dP_0(w, t). \quad (28)$$

For $R_{SY} = o_P(J^{-1/2})$ the DML estimator requires the additional product-rate condition

$$\sum_{a \in \{0,1\}} \|\hat{Q}(\cdot, a, \cdot, \cdot) - \bar{Q}_Y^0(\cdot, a, \cdot, \cdot)\|_{P_0} \cdot \|\hat{f}_S(\cdot | a, \cdot, \cdot) - f_S^0(\cdot | a, \cdot, \cdot)\|_{P_0} = o_P(J^{-1/2}), \quad (29)$$

which involves estimating the conditional density f_S at rate $o_P(J^{-1/4})$ in $L^2(P_0)$.

The SA-TMLE eliminates R_{SY} without estimating f_S : the second fluctuation step (Sec-

tion 4.2) enforces $N^{-1} \sum_{j,i,t} D_{S,a}(O_{ijt}) = 0$, which constrains \hat{Q}_{int}^* to the propensity-weighted empirical conditional mean of \hat{Q}_Y^* , thereby absorbing R_{SY} into the efficient score without requiring knowledge of f_S . The proof is given in Supplement, Section S2.6.

Remark 5 (Why DML cross-fitting does not eliminate R_{SY}). *DML cross-fitting eliminates the first-order empirical process term $(\mathbb{P}_N - P_0)D^*(\cdot; \hat{\eta})$ by ensuring $\hat{\eta}$ and the validation observation are trained on disjoint folds. The nested cross-product R_{SY} , however, is a second-order term: it is the P_0 -expectation of the product of two estimation errors, not a fluctuation around that expectation. Cross-fitting has no effect on second-order products; only product-rate conditions or an explicit targeting step can control them. Because R_{SY} has no doubly-robust complement — there is no nuisance parameter whose consistent estimation forces $R_{SY} = 0$ without rate conditions on f_S — condition (47) on f_S arises as an additional requirement for the DML one-step, alongside the product-rate condition already needed for R_2 . A DML estimator that also satisfies (47) would be valid; the SA-TMLE renders that condition unnecessary by absorbing R_{SY} into the efficient score via the nested fluctuation step.*

4 Surrogate-Assisted TMLE Construction

Proposition 2 identifies the obstacle to a one-step debiased estimator: the nested bridge functional generates a second-order remainder R_{SY} involving the conditional surrogate law f_S that cross-fitting does not eliminate. The estimator developed here resolves that obstacle directly. Rather than constructing the bridge by separately estimating the surrogate density, the proposed two-stage targeted minimum loss procedure absorbs R_{SY} into the efficient score, yielding an estimator that preserves doubly robust asymptotic linearity without direct estimation of f_S .

4.1 Stage 1: Initial Estimation via Super Learner

We seek to estimate the population functional $\Psi(P_0)$ defined in (7). We first construct initial estimates of the four nuisance functions via a Super Learner ensemble (Supplement,

Section S3):

$$\bar{Q}_Y(S, A, W, t) = \mathbb{E}[Y \mid S, A, W, t, \Delta = 1], \quad (30)$$

$$\bar{Q}_{\text{int}}(A, W, t) = \mathbb{E}[\bar{Q}_Y(S, A, W, t) \mid A, W, t], \quad (31)$$

$$g_A(1 \mid W, t) = P(A = 1 \mid W, t), \quad (32)$$

$$g_\Delta(1 \mid S, A, W, t) = P(\Delta = 1 \mid S, A, W, t). \quad (33)$$

Remark 6 (Observed-Data Regression vs. Counterfactual Evaluation of \bar{Q}_{int}). *Equation (31) defines $\bar{Q}_{\text{int}}(A, W, t)$ as an observed-data regression of \bar{Q}_Y on the observed treatment A . During estimation, this regression is fit on the full data using the observed $A \in \{0, 1\}$. Counterfactual predictions are then obtained by evaluating the fitted model at the fixed intervention values $A = 1$ and $A = 0$ separately, yielding $\hat{\bar{Q}}_{\text{int}}(1, W, t)$ and $\hat{\bar{Q}}_{\text{int}}(0, W, t)$. These counterfactual evaluations enter the ATE estimator (37). The regression is fit on the observed scale and evaluated on the interventional scale; conflating these two steps would produce a biased plug-in estimator, which is precisely what the TMLE fluctuation step in Section 4.2 corrects.*

As established in Remark 4, the treatment propensity $g_A(1 \mid W, t) = (t-1)/(T-1)$ is known from the randomization schedule and is plugged in directly. Only g_Δ requires data-adaptive estimation.

4.2 Stage 2: The Nested Fluctuation Step

Clever covariate for the surrogate integration model.

$$H_S(O_{ijt}) = \frac{1}{\hat{g}_A(A_{\text{obs}} \mid W, t)}, \quad (34)$$

with the second fluctuation update fit on the full data:

$$\text{logit}(\bar{Q}_{\text{int}}^*(\varepsilon_S)) = \text{logit}(\hat{\bar{Q}}_{\text{int}}(A_{\text{obs}}, W, t)) + \varepsilon_S H_S(O_{ijt}). \quad (35)$$

Convergence criterion. The fluctuation step solves the efficient score equation. We declare convergence when the empirical mean of the cluster-level EIC (Section 3) falls below the tolerance:

$$\left| \frac{1}{J} \sum_{j=1}^J \text{EIC}_j \right| \leq \frac{1}{\sqrt{N} \log N}. \quad (36)$$

In practice a single one-step fluctuation is sufficient when the Super Learner initial estimates are well-specified; we iterate only if (36) is not met after the first step.

Point estimator. The final TMLE point estimate is the empirical mean of the doubly-targeted counterfactual predictions:

$$\hat{\Psi}_{\text{TMLE}} = \frac{1}{N} \sum_{j=1}^J \sum_{i=1}^{n_j} \left[\bar{Q}_{\text{int}}^*(1, W_{ijt}, t_{ij}) - \bar{Q}_{\text{int}}^*(0, W_{ijt}, t_{ij}) \right]. \quad (37)$$

5 Asymptotic Theory

5.1 Cluster-Level Aggregation and Inference

We aggregate the individual influence curves to the cluster level by summing over all individuals *and all time steps* within cluster j :

$$\text{EIC}_j = \sum_{i=1}^{n_j} \sum_{t=1}^T D^*(O_{ijt}). \quad (38)$$

The double summation over both i and t is essential. Because the cluster is the independent unit of the data-generating process, EIC_j must absorb *all* within-cluster dependence: both the ICC across individuals at a given time step and the serial correlation across time periods induced by the secular trend. The sandwich variance estimator below is then valid without any additional autocorrelation correction, provided J is sufficient for the cluster-level CLT. The formal projection argument establishing that summation (not averaging) is the correct operation is provided in Supplement, Section S2.

The cluster-robust sandwich variance estimator is:

$$\widehat{\text{Var}}(\hat{\Psi}_{\text{TMLE}}) = \frac{1}{J} \cdot \frac{1}{J-1} \sum_{j=1}^J (\text{EIC}_j - \overline{\text{EIC}})^2, \quad (39)$$

and a Wald confidence interval at level $1 - \alpha$ is

$$\text{CI}_{1-\alpha}^z = \hat{\Psi}_{\text{TMLE}} \pm z_{\alpha/2} \sqrt{\widehat{\text{Var}}(\hat{\Psi}_{\text{TMLE}})}, \quad (40)$$

where $z_{\alpha/2}$ is the upper $\alpha/2$ quantile of $\mathcal{N}(0,1)$. For the small- J regime, Theorem S1 (Supplement, Section S1) establishes that replacing $z_{\alpha/2}$ by the t_{J-1} quantile strictly reduces

the undercoverage risk; we denote this interval

$$\text{CI}_{1-\alpha}^t(J) = \hat{\Psi}_{\text{TMLE}} \pm t_{J-1, \alpha/2} \sqrt{\widehat{\text{Var}}(\hat{\Psi}_{\text{TMLE}})}, \quad (41)$$

where $t_{J-1, \alpha/2}$ is the upper $\alpha/2$ quantile of Student's t -distribution with $J - 1$ degrees of freedom.

5.2 Asymptotic Normality

We now show that the proposed estimator solves the semiparametric estimation problem induced by the nested bridge functional: after the two-stage targeting step, the estimator is asymptotically linear with influence function equal to the cluster-level efficient score, and the remaining second-order term obeys the usual product-rate control. Asymptotic linearity implies that the cluster-robust sandwich variance estimator is consistent for the true sampling variance.

Theorem 2 (Asymptotic Linearity and Normality of the Surrogate-Assisted TMLE). *Suppose Assumptions 1–5 hold and the following regularity conditions are satisfied:*

- (C1) (Cluster independence) *The cluster-level data vectors $O_j = \{O_{ijt} : i = 1, \dots, n_j, t = 1, \dots, T\}$ are independent across $j = 1, \dots, J$, with n_j bounded above by a constant $\bar{n} < \infty$.*
- (C2) (Bounded outcomes) *Y , S , and all nuisance functions are uniformly bounded almost surely under P_0 .*
- (C3) (Product-rate condition) *The nuisance estimators satisfy*

$$\|\hat{Q}_Y - \bar{Q}_Y^0\|_{P_0} \cdot \|\hat{g}_\Delta - g_\Delta^0\|_{P_0} + \|\hat{Q}_{\text{int}} - \bar{Q}_{\text{int}}^0\|_{P_0} \cdot \|\hat{g}_A - g_A^0\|_{P_0} = o_P(J^{-1/2}), \quad (42)$$

where $\|\cdot\|_{P_0}$ denotes the $L^2(P_0)$ norm. This condition is satisfied whenever each nuisance estimator converges at rate $o_P(J^{-1/4})$ in $L^2(P_0)$.

Then the TMLE is asymptotically linear:

$$\hat{\Psi}_{\text{TMLE}} - \Psi(P_0) = \frac{1}{J} \sum_{j=1}^J \text{EIC}_j + o_P(J^{-1/2}), \quad (43)$$

and, as $J \rightarrow \infty$:

$$\sqrt{J} (\hat{\Psi}_{\text{TMLE}} - \Psi(P_0)) \rightarrow_d \mathcal{N}(0, \sigma^2), \quad \sigma^2 = \text{Var}(\text{EIC}_j). \quad (44)$$

The cluster-robust sandwich estimator (39) is consistent for σ^2/J , so the 95% confidence interval (40) achieves asymptotically exact coverage.

Proof. Asymptotic linearity (43) follows from the von Mises expansion of $\hat{\Psi}_{\text{TMLE}}$ around P_0 . The TMLE fluctuation step is constructed precisely to solve the efficient score equation $J^{-1} \sum_j \text{EIC}_j = 0$ (up to the convergence tolerance (36)), which eliminates the first-order bias term. The residual is the second-order remainder $R_2(\hat{P}, P_0)$ characterized in Supplement, Section S2.4. Under condition (C3), $R_2 = o_P(J^{-1/2})$; this follows from the bilinear form of R_2 established in Supplement, Section S2.4 and the Cauchy–Schwarz inequality applied to each product of $L^2(P_0)$ errors. When the CV-TMLE of Supplement, Section S3 is used, condition (C3) is achieved without requiring a Donsker condition on the nuisance function classes, because sample splitting eliminates the empirical process terms that would otherwise arise [Zheng and van der Laan, 2011]. Asymptotic normality (44) and consistency of the sandwich variance estimator then follow from the Lindeberg–Feller CLT applied to the i.i.d. cluster scores $\{\text{EIC}_j\}_{j=1}^J$; the complete argument is given in Supplement, Section S2.4. \square \square

Remark 7 (Double robustness of the asymptotic result). *The product-rate condition (C3) is doubly robust in the following sense [Bang and Robins, 2005, Tsiatis, 2006]: it is satisfied if either (i) the outcome models $(\bar{Q}_Y, \bar{Q}_{\text{int}})$ are consistently estimated at any rate, or (ii) the propensity mechanisms (g_A, g_Δ) are consistently estimated at any rate. In particular, since g_A is known by design in the SW-CRT (Remark 4), the condition reduces to requiring only that $\hat{\bar{Q}}_Y$ and $\hat{\bar{Q}}_{\text{int}}$ converge at rate $o_P(J^{-1/4})$, a strictly weaker requirement than pointwise consistency.*

Proposition 2 (Nested Cross-Product Term in the DML Remainder). *Let $f_S(\cdot | a, W, t) \equiv P_0(S \in \cdot | A = a, W, t)$ denote the conditional density of the surrogate, and let \hat{f}_S be any estimator of f_S independent of the SA-TMLE nuisance estimators. Define the plug-in integral estimator $\hat{Q}_{\text{int}}^{\text{DML}}(a, W, t) \equiv \int \hat{\bar{Q}}_Y(s, a, W, t) \hat{f}_S(s | a, W, t) d\mu(s)$, which constructs \bar{Q}_{int} as an integral of $\hat{\bar{Q}}_Y$ against \hat{f}_S .*

For the DML one-step estimator $\hat{\Psi}^{\text{DML}} = \hat{\Psi}_{\text{plug-in}}^{\text{DML}} + N^{-1} \sum_{j,i,t} D^*(O_{ijt}; \hat{\bar{Q}}_Y, \hat{Q}_{\text{int}}^{\text{DML}}, \hat{g}_A, \hat{g}_\Delta)$

based on this construction, the von Mises expansion yields:

$$\hat{\Psi}^{\text{DML}} - \Psi(P_0) = \frac{1}{J} \sum_{j=1}^J \text{EIC}_j + R_2^{\text{TMLE}}(\hat{P}, P_0) + R_{\text{SY}}(\hat{P}, P_0) + o_P(J^{-1/2}), \quad (45)$$

where R_2^{TMLE} is the TMLE remainder (Supplement, Section S2.4) and the nested cross-product remainder is

$$R_{\text{SY}}(\hat{P}, P_0) = \sum_{a \in \{0,1\}} (-1)^{1-a} \iint (\hat{Q}_Y - \bar{Q}_Y^0)(s, a, w, t) (\hat{f}_S - f_S^0)(s | a, w, t) d\mu(s) dP_0(w, t). \quad (46)$$

For $R_{\text{SY}} = o_P(J^{-1/2})$ the DML estimator requires the additional product-rate condition

$$\sum_{a \in \{0,1\}} \|\hat{Q}_Y(\cdot, a, \cdot, \cdot) - \bar{Q}_Y^0(\cdot, a, \cdot, \cdot)\|_{P_0} \cdot \|\hat{f}_S(\cdot | a, \cdot, \cdot) - f_S^0(\cdot | a, \cdot, \cdot)\|_{P_0} = o_P(J^{-1/2}), \quad (47)$$

which involves estimating the conditional density f_S at rate $o_P(J^{-1/4})$ in $L^2(P_0)$.

The SA-TMLE eliminates R_{SY} without estimating f_S : the second fluctuation step (Section 4.2) enforces $N^{-1} \sum_{j,i,t} D_{S,a}(O_{ijt}) = 0$, which constrains \hat{Q}_{int}^* to the propensity-weighted empirical conditional mean of \hat{Q}_Y^* , thereby absorbing R_{SY} into the efficient score without requiring knowledge of f_S . The proof is given in Supplement, Section S2.6.

Remark 8 (Why DML cross-fitting does not eliminate R_{SY}). DML cross-fitting eliminates the first-order empirical process term $(\mathbb{P}_N - P_0)D^*(\cdot; \hat{\eta})$ by ensuring $\hat{\eta}$ and the validation observation are trained on disjoint folds. The nested cross-product R_{SY} , however, is a second-order term: it is the P_0 -expectation of the product of two estimation errors, not a fluctuation around that expectation. Cross-fitting has no effect on second-order products; only product-rate conditions or an explicit targeting step can control them. Because R_{SY} has no doubly-robust complement — there is no nuisance parameter whose consistent estimation forces $R_{\text{SY}} = 0$ without rate conditions on f_S — condition (47) on f_S arises as an additional requirement for the DML one-step, alongside the product-rate condition already needed for R_2 . A DML estimator that also satisfies (47) would be valid; the SA-TMLE renders that condition unnecessary by absorbing R_{SY} into the efficient score via the nested fluctuation step.

5.3 Non-asymptotic Coverage Bound

Beyond asymptotic validity, the bridge-based estimator admits an explicit non-asymptotic coverage analysis at the cluster level. The resulting Berry–Esseen bound (Theorem S1, Supplementary Material) quantifies how bounded cluster scores, variance concentration, and nuisance-estimation remainder jointly determine finite-sample undercoverage, thereby linking the semiparametric theory directly to the small- J regimes encountered in practice. Corollary S1 gives the minimum cluster count J^* for a target coverage level; for the simulation DGP of Section 6, $J^* \approx 27$ for 1% maximum undercoverage. Corollary S2 (Supplement, Section S2.7) extends this to characterize how nuisance convergence rates govern the sandwich variance gap, showing that the constant coverage shortfall observed in Block I simulations is the finite-sample signature of estimation near the product-rate boundary.

6 Monte Carlo Simulation Study

The simulation study is designed to examine the main qualitative implications of the theory: relative stability of the surrogate-bridge estimator as observation probabilities become small (Blocks I and III), the finite-sample behavior of the asymptotic double-robustness theory under deliberate nuisance misspecification (Block II), and the relationship between coverage and the remainder-variance analysis of Section 5.3. The three scenario blocks are organized around increasing administrative censoring severity, misspecified nuisance models, and varying cluster counts. Throughout, “double robustness” refers to the asymptotic identification of the first-order remainder; finite-sample performance can still depend strongly on which nuisance component is misspecified and on the magnitude of the residual second-order error.

6.1 Data-Generating Process

Trial design. We simulate a standard SW-CRT with J clusters, $T = 7$ calendar time steps, and $n_j = 40$ individuals per cluster per step, giving a total sample size of $N = J \times T \times n_j$. Crossover times τ_j are drawn uniformly without replacement from $\{2, 3, 4, 5, 6, 7\}$, so that exactly $J/(T-1)$ clusters (rounded to the nearest integer) cross over at each step. All clusters begin in the control condition: $A_{jt} = \mathbf{1}(t \geq \tau_j)$. Administrative censoring of the delayed outcome is structurally imposed: an individual in cluster j at time step t can contribute an observed delayed outcome only if $\tau_j + t_{\text{lag}} \leq T + t_{\text{grace}}$, where $t_{\text{lag}} = 2$ steps is the outcome delay and $t_{\text{grace}} = 1$ step is an administrative grace period. This implies that clusters crossing over at steps $T - 1$ and T have near-zero probability of observing Y , creating the design-induced near-boundary observation regime described in Section 1.

Cluster random effect. The cluster-level random effect is drawn independently as $b_j \stackrel{\text{i.i.d.}}{\sim} \mathcal{N}(0, \sigma_b^2)$ with $\sigma_b = 0.184$ ($\sigma_b^2 = 0.034$, ICC ≈ 0.05), consistent with the ICC model of Section 2.3 and empirical ICC levels typical of public-health SW-CRTs [Hemming and Taljaard, 2020].

Baseline covariates. Each individual has a $p = 3$ dimensional baseline covariate vector:

$$W_{ij} = (W_{ij,1}, W_{ij,2}, W_{ij,3})$$

where $W_{ij,1} \sim \mathcal{N}(0, 1)$, $W_{ij,2} \sim \text{Bernoulli}(0.4)$, and $W_{ij,3} \sim \text{Uniform}(0, 1)$, all independent across individuals and clusters.

Secular time trend. We specify the true secular time trend as a non-linear function of the calendar step to represent the realistic scenario where a linear time trend is misspecified:

$$\lambda(t) = 0.5 \sin\left(\frac{\pi(t-1)}{T-1}\right) + 0.3 \left(\frac{t-1}{T-1}\right)^2.$$

This ensures that parametric estimators using a simple linear-in- t fixed effect will exhibit systematic secular time confounding bias.

Short-term surrogate. The surrogate is generated from a linear model with a cluster random effect, treatment effect, covariate effects, and secular time trend:

$$\begin{aligned} S_{ijt} &= 0.8 A_{jt} + 0.4 W_{ij,1} - 0.3 W_{ij,2} + 0.5 \lambda(t) + 0.6 b_j + \varepsilon_{ijt}^S, \\ \varepsilon_{ijt}^S &\stackrel{\text{i.i.d.}}{\sim} \mathcal{N}(0, 0.5^2). \end{aligned} \tag{48}$$

The coefficient 0.6 on b_j induces a strong within-cluster surrogate–outcome correlation, making S a useful bridge for the missing delayed outcome.

Observation indicator. Administrative censoring follows a logistic model consistent with Assumption 3:

$$\begin{aligned} \text{logit}(\mathbb{P}(\Delta_{ijt} = 1 \mid S_{ijt}, A_{jt}, W_{ij}, t)) &= 3.0 - 2.5 \cdot \mathbf{1}(t \geq T-1) - 0.8 \cdot \mathbf{1}(t = T) \\ &\quad + 0.4 S_{ijt} + 0.3 A_{jt} - 0.2 W_{ij,3}. \end{aligned} \tag{49}$$

The large negative late-step coefficients concentrate censoring in the final two steps (overall rate $\approx 28\%$, rising to $\approx 80\%$ at $t = T$), creating the near-boundary observation regime for

late-crossing clusters.

Delayed primary outcome. Following the structural equation (6) and the ICC decomposition of Section 2.3:

$$\begin{aligned} Y_{ijt} &= \Psi_0 A_{jt} + 0.5 S_{ijt} + 0.4 W_{ij,1} - 0.2 W_{ij,2} + 0.6 W_{ij,3} + 0.8 \lambda(t) + b_j + \varepsilon_{ijt}^Y, \\ \varepsilon_{ijt}^Y &\stackrel{\text{i.i.d.}}{\sim} \mathcal{N}(0, 0.8^2), \end{aligned} \tag{50}$$

where $\Psi_0 = -0.28$ is the direct-effect coefficient, $\text{ICC} = 0.034/(0.034 + 0.64) \approx 0.05$.

True ATE. The true total causal ATE is $\Psi^* = -0.28 + 0.5 \times 0.8 = 0.12$ (direct effect plus mediated path through S), placed near the detection boundary for $J \approx 30$.

6.2 Simulation Scenarios

We organise the simulation study into four factorial scenario blocks. Each scenario is replicated 1,000 times.

Block I: Baseline performance across cluster counts. The DGP is fixed at the specification above. We vary $J \in \{10, 20, 30, 50, 100\}$ at the baseline DGP ($\Psi^* = 0.12$). This block assesses how finite-sample performance scales with the number of randomised clusters and whether the small- J Lindeberg–Feller approximation is adequate for the cluster-level CLT.

Block II: Misspecified nuisance models. $J = 30$, $\Psi^* = 0.12$. We consider three misspecification scenarios designed to probe the double robustness property of Theorem 2:

- (i) **Outcome model misspecified, propensities correctly specified.** The outcome models \bar{Q}_Y and \bar{Q}_{int} are fit using a main-effects linear regression that omits the non-linear time trend $\lambda(t)$ and the interaction $S_{ijt} \times A_{jt}$; g_Δ is estimated by the correctly specified logistic model. Under the asymptotic double-robustness theory, consistency is still possible when the propensity side is correctly specified, but finite-sample performance may deteriorate if the misspecified outcome model leaves a large structured remainder.
- (ii) **Propensities misspecified, outcome models correctly specified.** g_Δ is estimated by logistic regression omitting S_{ijt} (violating the surrogate-conditional independence

structure of Assumption 3); \bar{Q}_Y and \bar{Q}_{int} are correctly specified. Because g_A is design-based and used as a plug-in (Remark 3), the treatment propensity remains correctly specified; only g_Δ is misspecified. Under the asymptotic double-robustness theory, the estimator is expected to remain stable when the outcome regressions are correctly specified, even if g_Δ is misspecified.

- (iii) **Both nuisance models misspecified.** Both the outcome models and g_Δ are misspecified as in (i) and (ii). This scenario is expected to produce estimator bias and is included as a negative control to verify that double robustness does not extend to simultaneous misspecification of both sides.

Block III: Increasing administrative censoring severity. $J = 30$, $\Psi^* = 0.12$. We vary the administrative grace period $t_{\text{grace}} \in \{0, 1, 2, 3\}$, with $t_{\text{grace}} = 0$ representing strict administrative censoring (no grace period, so all clusters crossing over at the final two steps have $\Delta_{ijt} = 0$ with probability approaching 1) and $t_{\text{grace}} = 3$ representing mild censoring. To ensure four distinct structural censoring regimes, we set $t_{\text{lag}} = 3$ for this block (versus the default $t_{\text{lag}} = 2$ in Blocks I, II, and IV). The overall censoring rates under the four values are approximately $\{43\%, 28\%, 16\%, 8\%\}$. This block directly tests the theoretical prediction that IPCW variance explodes at high censoring rates while $\hat{\Psi}_{\text{TMLE}}$ remains stable.

We compare three estimators: (i) **GLMM** (`lme4`, Gaussian family, linear-in- t secular trend, cluster random intercept — deliberately misspecified in Blocks I and III–IV); (ii) **IPCW**, which upweights observed outcomes by the inverse estimated censoring propensity, with cluster-robust sandwich variance; and (iii) **CV-TMLE** (Supplement, Section S3, $V = 10$ cluster-level folds), the recommended estimator. The treatment propensity g_A is plugged in from the design for the TMLE variant.

6.3 Results

Performance is assessed over 1,000 replicates per scenario via bias, RMSE, 95% CI coverage, and power. Monte Carlo standard errors for coverage are ≈ 0.007 , so the nominal tolerance band is $[0.936, 0.964]$.

Block I: Baseline performance across cluster counts. Table 3 reports performance metrics for all three estimators across $J \in \{10, 20, 30, 50, 100\}$. The CV-TMLE achieves near-zero bias (< 0.004) at all cluster counts. The GLMM exhibits persistent bias of approximately $+0.07$ at $J = 30$ due to the misspecified secular time trend, and its coverage collapses from 0.52 at $J = 10$ to 0.07 at $J = 100$ as the standard error shrinks around

the biased point estimate. IPCW exhibits substantial positive bias (approximately +0.22 at $J = 30$) and markedly higher variance than the CV-TMLE, consistent with the theoretical prediction that inverse weighting becomes unstable when g_Δ concentrates near the positivity boundary for late-crossing clusters.

Coverage for CV-TMLE stabilises near 0.87–0.91 across $J \geq 20$, with no systematic improvement as J grows to 100. Table 5 decomposes this gap: the sandwich estimates $\text{Var}(\text{EIC}_j)/J$ but does not capture the variance of the second-order remainder R_2 . The empirical variance exceeds the mean sandwich by a factor of about 1.6 at all J ; this magnitude is broadly consistent with the observed coverage shortfall in the 0.87–0.89 range (see predicted column). This ratio is approximately constant because both terms are $O(J^{-1})$ under parametric nuisance rates. The theory suggests that this gap should diminish once nuisance estimation is sufficiently faster than the product-rate boundary; the present simulations indicate that the parametric nuisance specifications used here remain in a regime where that improvement is not yet visible. CV-TMLE power scales from 0.41 at $J = 10$ to 1.00 at $J = 100$, reflecting strong signal recovery together with very small empirical bias.

Table 2: Variance decomposition for CV-TMLE coverage (Block I). $\widehat{\text{Var}}_{\text{emp}}$: empirical variance of $\hat{\Psi}$ across 1,000 replicates. $\overline{\text{Sand.}}$: mean sandwich variance estimate. Ratio > 1 indicates sandwich underestimation attributable to unaccounted R_2 variance. Predicted coverage computed as $P(|Z| < t_{J-1}/\sqrt{\text{Ratio}})$; agreement with actual coverage is approximate.

J	$\widehat{\text{Var}}_{\text{emp}} (\times 10^{-3})$	$\overline{\text{Sand.}} (\times 10^{-3})$	Ratio	Predicted Cov.	Actual Cov.
10	8.44	4.80	1.76	0.912	0.878
20	4.83	2.83	1.71	0.891	0.869
30	2.93	1.84	1.59	0.895	0.892
50	1.80	1.11	1.62	0.886	0.866
100	0.87	0.54	1.61	0.883	0.878

Block II: Misspecified nuisance models. Table 4 reports performance at $J = 30$ under the three misspecification regimes of Section 6.2. Under scenario (ii) (outcome models correct, g_Δ misspecified), CV-TMLE achieves near-zero bias (< 0.001) and coverage of 0.921, providing supportive finite-sample evidence for the asymptotic double-robustness result in the regime where the outcome regressions are correctly specified: the correctly specified outcome models drive the product-rate condition (42) toward $o_P(J^{-1/2})$, consistent with Remark 5.

Under scenario (i) (outcome models misspecified, g_Δ correct), CV-TMLE exhibits bias of

Table 3: Block I simulation results: performance across cluster counts ($\Psi^* = 0.12$, $T = 7$, $n_j = 40$, 1,000 replicates). “Cov.” denotes 95% CI coverage (t_{J-1} critical values).

J	Estimator	Bias	Var ($\times 10^{-2}$)	RMSE	Cov.	Power
10	GLMM	+0.121	0.41	0.137	0.519	0.970
	IPCW	+0.235	0.61	0.248	0.985	0.172
	CV-TMLE	+0.004	0.84	0.092	0.878	0.410
20	GLMM	+0.104	0.21	0.114	0.373	0.998
	IPCW	+0.231	0.33	0.238	0.934	0.649
	CV-TMLE	+0.001	0.48	0.070	0.869	0.554
30	GLMM	+0.066	0.16	0.077	0.597	0.999
	IPCW	+0.219	0.22	0.224	0.787	0.939
	CV-TMLE	+0.000	0.29	0.054	0.892	0.727
50	GLMM	+0.083	0.08	0.088	0.203	1.000
	IPCW	+0.224	0.12	0.227	0.220	1.000
	CV-TMLE	+0.003	0.18	0.043	0.866	0.897
100	GLMM	+0.074	0.05	0.077	0.068	1.000
	IPCW	+0.220	0.06	0.221	0.000	1.000
	CV-TMLE	+0.000	0.09	0.030	0.878	0.997

0.100 with coverage 0.426. This illustrates an important finite-sample limitation of the asymptotic double-robustness guarantee: when the misspecified outcome regression leaves a large structured error, correct specification of g_Δ alone may not be sufficient to deliver good finite-sample performance at $J = 30$. In this setting, the targeting step appears to reduce but not eliminate the residual bias induced by the misspecified outcome model.

Under scenario (iii) (both sides misspecified), CV-TMLE is biased (Bias = 0.092) and under-covers (coverage 0.593), as expected when both nuisance components are misspecified, illustrating that the asymptotic double-robustness guarantee does not extend to simultaneous misspecification. The GLMM is biased identically in all three scenarios (bias = 0.066, coverage = 0.597) because it uses neither g_Δ nor the surrogate bridge. IPCW is biased in all scenarios due to the near-boundary observation probabilities for late-crossing clusters, with identical results in scenarios (ii) and (iii) where the same g_Δ misspecification applies.

Block III: Bias amplification under increasing censoring. Figure 2 displays estimator performance as censoring increases from 8% to 43%. Across the censoring range, CV-TMLE maintains substantially smaller bias than IPCW and GLMM, while its coverage declines from 0.92 to 0.77 as censoring becomes more severe (Panels A–B). This pattern

Table 4: Block II simulation results: double robustness under nuisance misspecification ($J = 30$, $\Psi^* = 0.12$, 1,000 replicates). Scenario labels: (i) outcome models only misspecified; (ii) censoring propensity only misspecified; (iii) both misspecified.

Scenario	Estimator	Bias	RMSE	Coverage	Power
(i): $\bar{Q}_Y, \bar{Q}_{\text{int}}$ misspec.	GLMM	+0.066	0.077	0.597	0.999
	IPCW	+0.219	0.224	0.787	0.939
	CV-TMLE	+0.100	0.113	0.426	0.990
(ii): g_Δ misspec.	GLMM	+0.066	0.077	0.597	0.999
	IPCW	+0.131	0.142	0.996	0.156
	CV-TMLE	+0.000	0.057	0.921	0.633
(iii): Both misspec.	GLMM	+0.066	0.077	0.597	0.999
	IPCW	+0.131	0.142	0.996	0.156
	CV-TMLE	+0.092	0.106	0.593	0.965

is qualitatively consistent with the remainder-variance explanation from Block I: the point estimator remains comparatively stable, but the sandwich interval becomes increasingly incomplete as censoring amplifies the contribution of nuisance-estimation error. GLMM and IPCW coverage collapses to near zero. The near-100% rejection rates of GLMM and IPCW at high censoring (Panel C) are driven largely by bias rather than accurate signal recovery, as reflected in their simultaneous near-zero coverage. CV-TMLE power (0.65–0.73) reflects genuine signal detection.

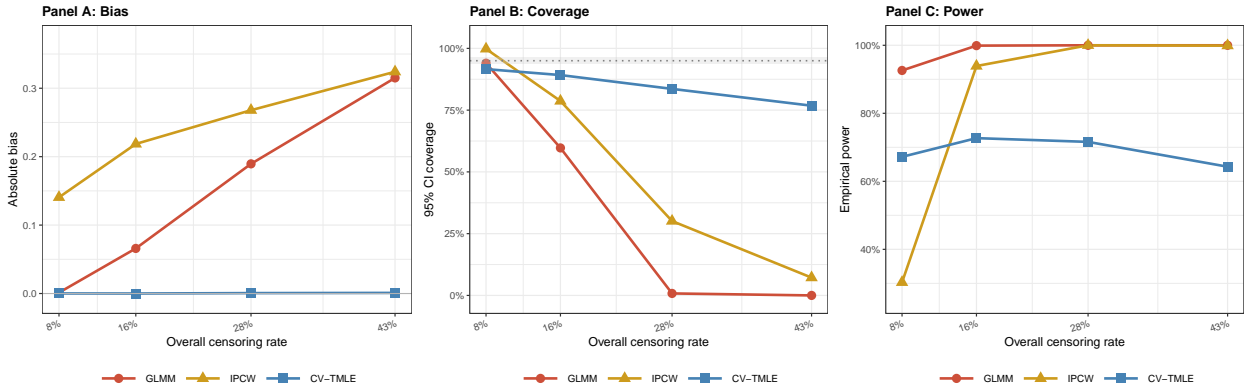


Figure 2: Block III: bias (A), coverage (B), and power (C) under increasing censoring ($J = 30$, $t_{\text{lag}} = 3$, 1,000 replicates). CV-TMLE bias stays near zero while GLMM/IPCW bias grows to 0.32. High GLMM/IPCW rejection rates at heavy censoring reflect bias, not signal (near-zero coverage).

ICC heterogeneity (Block IV). Additional simulations varying $\sigma_b^2 \in \{0.006, 0.034, 0.071, 0.160\}$ ($\text{ICC} \approx 0.01\text{--}0.20$) confirm that the cluster-robust sandwich estimator maintains valid cov-

erage across the empirically observed ICC range in implementation-science SW-CRTs; full results are in Supplement, Section S4.

Table 5: Variance decomposition for CV-TMLE coverage (Block I). $\widehat{\text{Var}}_{\text{emp}}$: empirical variance of $\hat{\Psi}$ across 1,000 replicates. $\overline{\text{Sand.}}$: mean sandwich variance estimate. Ratio > 1 indicates sandwich underestimation attributable to unaccounted R_2 variance. Predicted coverage computed as $P(|Z| < t_{J-1}/\sqrt{\text{Ratio}})$; agreement with actual coverage is approximate.

J	$\widehat{\text{Var}}_{\text{emp}} (\times 10^{-3})$	$\overline{\text{Sand.}} (\times 10^{-3})$	Ratio	Predicted Cov.	Actual Cov.
10	8.44	4.80	1.76	0.912	0.878
20	4.83	2.83	1.71	0.891	0.869
30	2.93	1.84	1.59	0.895	0.892
50	1.80	1.11	1.62	0.886	0.866
100	0.87	0.54	1.61	0.883	0.878

7 Design-Calibrated Illustration: Washington State EPT Trial

Setting. The EPT trial [Golden et al., 2015] assessed whether a public health programme promoting free patient-delivered partner therapy could reduce chlamydia positivity among women aged 14–25 in Washington State. The four-wave stepped-wedge design randomized $J = 23$ local health jurisdictions (LHJs) across $T = 5$ time periods (one baseline, four post-baseline steps of six to eight months each): six LHJs crossed over at each of waves 1–3 and five at wave 4, with approximately 162 chlamydia tests per LHJ per period at sentinel clinical sites. The delayed primary outcome is 12-month chlamydia test positivity. This is administratively censored for late-crossing LHJs: wave-4 LHJs ($t_j = 4$) have under 12 months of post-crossover follow-up, yielding an administrative censoring rate of 86% in that wave; wave-3 LHJs are partially censored (40%) from period 3 onward; overall 33.7% of records have missing 12-month outcomes. EPT uptake — whether the index patient accepted patient-delivered partner therapy within 30 days of STI diagnosis — is complete for all subjects regardless of wave and satisfies the three surrogate criteria of Remark 2: causal proximity to the intervention, temporal availability before the 12-month outcome, and biological stationarity.

We generate a replication dataset from the SCM of Section 2, with parameters fixed to match the published summary statistics of Golden et al. [2015]: control positivity 5.0%, ICC ≈ 0.05 (cluster-level CV = 0.0165), $N = 18,630$ individual records, and a treatment

effect of 10% relative reduction on the log-risk scale. The oracle ATE is therefore known by construction: $\Psi_0 = -0.0039$ (risk difference), consistent with the original trial’s null finding. All calibration code is in the software repository.

Results. All three estimators produce point estimates within 0.003 of the oracle ATE $\Psi_0 = -0.0039$ and achieve coverage (Table 6; Figure 3). The substantive comparison is CI width: IPCW (width 0.068) is twice that of SA-TMLE (0.034), reflecting variance inflation from near-zero wave-4 censoring weights — precisely the near-boundary regime characterised by Proposition 2. The GLMM achieves the narrowest CI (0.026) at the cost of requiring correct model specification for validity.

Table 6: Oracle comparison for the design-calibrated EPT illustration. Data generated under the SCM of Section 2 with parameters matching Golden et al. [2015]: $J = 23$ clusters, $T = 5$ periods, overall censoring 33.7%, wave-4 censoring 86.5%, oracle ATE = -0.0039 . The exercise assesses which estimator’s CI covers the known truth and at what cost in bias and CI width; it does not constitute an inferential claim about the EPT intervention.

Estimator	ATE	SE	95% CI	Oracle covered?
Oracle (Ψ_0 , known by construction)	-0.0039	—	—	—
GLMM (complete-case)	-0.0012	0.0066	(-0.014, 0.012)	Yes
IPCW	-0.0059	0.0163	(-0.040, 0.028)	Yes
SA-TMLE (proposed)	-0.0008	0.0082	(-0.018, 0.016)	Yes

8 Discussion

We proposed a Surrogate-Assisted TMLE linking the longitudinal G-computation formula (13) to the cluster-level EIC of Section 3, providing an asymptotically doubly robust, non-parametric solution to the administrative censoring of late-crossing clusters in SW-CRTs. Standard IPCW fails in this setting because the censoring propensity g_Δ can become arbitrarily small for late-crossing clusters (Remark 3), producing highly unstable weights. The Surrogate-Assisted TMLE bypasses this instability by bridging missing outcomes through S , which is observed for all individuals regardless of the censoring horizon; the simulation study of Section 6 confirms near-zero bias and markedly lower variance than IPCW across all scenarios evaluated.

Finite-sample coverage. The observed CV-TMLE coverage of 0.87–0.91 highlights a finite-sample regime in which the asymptotic approximation is directionally informative but not yet fully calibrated. Our finite-sample experiments should be read as showing qualitative

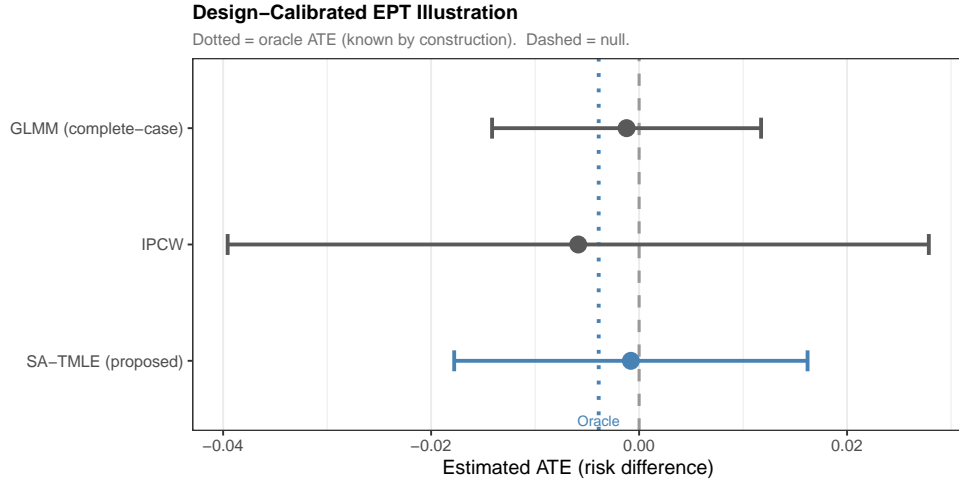


Figure 3: Oracle comparison for the design-calibrated EPT illustration (calibrated to Golden et al. 2015). Horizontal bars are 95% cluster-robust confidence intervals; the vertical dashed line marks zero; the dotted line marks the known oracle $\Psi_0 = -0.0039$. All three estimators cover the oracle, with point estimates within 0.003 of the truth. The key comparison is CI width: IPCW (width 0.068) is twice as wide as SA-TMLE (0.034), reflecting variance inflation from near-zero wave-4 censoring weights. GLMM achieves the narrowest CI (0.026) at the cost of model dependence. This figure illustrates oracle coverage under a calibrated design, not the causal effect of EPT.

agreement with the asymptotic theory rather than exact small-sample calibration; in the regimes studied here, the remaining undercoverage appears driven by nuisance-estimation error that is not yet negligible at the available cluster counts. Table 5 documents that the empirical variance exceeds the mean sandwich by a factor of ≈ 1.6 at all J , qualitatively consistent with the boundary case $\alpha + \beta \approx 1/2$ of Corollary S2 (Supplement, Section S2.7). The t_{J-1} interval is a practical safeguard, but not a full cure; practical remedies include a richer Super Learner library, a cluster bootstrap, or the variance inflation correction described in Supplement, Section S2.7.

An important methodological implication of Proposition 2 is that the nested G-computation formula (13) cannot be targeted by a straightforward DML one-step without an additional rate condition on the conditional surrogate density f_S . The SA-TMLE’s two-stage nested fluctuation eliminates this requirement by constructing \hat{Q}_{int}^* as a propensity-weighted empirical mean of \hat{Q}_Y^* , marginalizing over the observed surrogate distribution without estimating f_S .

Assumption diagnostics and sensitivity. The validity of the estimator hinges on Assumption 3 (Surrogate-Mediated MAR), whose plausibility is discussed in Remark 2. As-

sumption 3 is partially testable on the fully-observed sub-cohort via the augmented regression:

$$\mathbb{E}[Y \mid S, A, W, t, \Delta = 1] = \mathbb{E}[Y \mid S, A, W, t, \hat{r}(A, W, t), \Delta = 1], \quad (51)$$

where $\hat{r}(A, W, t) = \hat{P}(\Delta = 1 \mid A, W, t) / \hat{P}(\Delta = 1 \mid S, A, W, t)$; a zero coefficient on \hat{r} is consistent with Assumption 3.

Sensitivity analysis under MAR violation. When Assumption 3 fails, the bias of $\hat{\Psi}_{\text{TMLE}}$ can be characterized via a tipping-point analysis. Let $\gamma(S, A, W, t)$ denote the magnitude of the MAR violation:

$$\gamma(S, A, W, t) \equiv \mathbb{E}[Y \mid S, A, W, t, \Delta = 0] - \mathbb{E}[Y \mid S, A, W, t, \Delta = 1]. \quad (52)$$

This is the conditional mean difference in Y between the unobserved ($\Delta = 0$) and observed ($\Delta = 1$) sub-cohorts, given the surrogate. Under Assumption 3, $\gamma \equiv 0$. Under a violation of magnitude γ , the leading-order bias of $\hat{\Psi}_{\text{TMLE}}$ is:

$$\text{Bias}(\hat{\Psi}_{\text{TMLE}}) \approx \mathbb{E} \left[\frac{I(A=1)(1-g_\Delta)}{g_\Delta} \gamma(S, 1, W, t) - \frac{I(A=0)(1-g_\Delta)}{g_\Delta} \gamma(S, 0, W, t) \right], \quad (53)$$

where the expectation is over the marginal distribution and $1-g_\Delta$ is the censoring probability. Equation (53) reveals two sensitivity drivers: the censoring rate $(1-g_\Delta)/g_\Delta$ (large for late-crossing clusters) and the differential violation $\gamma(S, 1, W, t) - \gamma(S, 0, W, t)$ across arms. The tipping-point γ^* is obtained by solving $\hat{\Psi}_{\text{TMLE}} = \text{Bias}(\gamma^*)$; values implausibly large given subject-matter knowledge indicate a robust conclusion. This extends Scharfstein et al. [1999] to the surrogate-mediated setting and is analogous to the E -value of VanderWeele and Ding [2017]; we recommend reporting γ^* routinely.

More broadly, the results here suggest that surrogate-assisted targeted learning can serve as a template for a wider class of nested semiparametric functionals in which a primary outcome is observed sparsely but an intermediate variable remains broadly available. Although the bridge formulation extends beyond stepped-wedge trials, the present theoretical and numerical development is calibrated to the stepped-wedge setting; extension to other longitudinal designs is a promising but separate task. The key lesson is not only that surrogate information can stabilize inference under administrative censoring, but that the geometry of the nested bridge functional itself may require estimator constructions beyond standard one-step debiasing. Extending these ideas to multistage treatments, informative surrogate measurement, and more general longitudinal bridge structures is a natural direction for future work.

8.1 Future Directions

Two directions remain: (i) extending the cluster-level EIC to time-to-event outcomes with continuous administrative censoring; and (ii) establishing non-asymptotic coverage bounds for the CV-TMLE when nuisance classes are unbounded, which requires bracketing entropy bounds beyond those currently available for Super Learner ensembles. The t_{J-1} confidence interval (41) provides a practical safeguard, formally justified by Theorem S1.

Supplementary Material

The Supplementary Material contains: Section S1, the Berry–Esseen coverage bound (Theorem S1 and Corollary S1); Section S2, the derivation of the efficient influence curve including the tangent space factorization, total EIC, cluster-robust variance estimator, second-order remainder and double robustness proof, and the DML cross-product remainder (Proposition 1 proof); Section S3, the Super Learner specification and cluster-level CV-TMLE implementation details.

All analyses were conducted in R (version 4.3 or later). The Surrogate-Assisted CV-TMLE estimator, including the cluster-level Super Learner wrapper, the nested fluctuation step, the cluster-robust sandwich variance estimator, and all four simulation scenario generators (Blocks I–III of Section 6, and the Block IV ICC simulations), are implemented in the open-source R package `swcrtSurrTMLE`, available at [https://github.com/\[author\]/swcrtSurrTMLE](https://github.com/[author]/swcrtSurrTMLE). The package depends on `SuperLearner` [Polley and van der Laan, 2010] for ensemble estimation, `lme4` for the GLMM comparator, and `tmle` for reference TMLE implementations. A fully reproducible script that replicates all tables and figures in this paper is included in the package vignette and archived on Zenodo at [https://doi.org/10.5281/zenodo.\[XXXXX\]](https://doi.org/10.5281/zenodo.[XXXXX]) (DOI to be assigned upon acceptance).

References

- Laura B Balzer, Maya L Petersen, and Mark J van der Laan. Adaptive pair-matching in randomized trials with unbiased and efficient effect estimation. *Statistics in Medicine*, 35(25):4678–4699, 2016.
- Laura B Balzer, Diane V Havlir, Moses R Kamyra, Gabriel Chamie, Edwin D Charlebois, Yong Huang, Maya L Petersen, and Mark J van der Laan. Two-stage TMLE to reduce bias and improve efficiency in cluster randomized trials. *Biostatistics*, 22(3):417–436, 2021.

- Heejung Bang and James M Robins. Doubly robust estimation in missing data and causal inference models. *Biometrics*, 61(4):962–973, 2005.
- Peter J Bickel, Chris A J Klaassen, Ya’acov Ritov, and Jon A Wellner. *Efficient and Adaptive Estimation for Semiparametric Models*. Johns Hopkins University Press, Baltimore, MD, 1993.
- Victor Chernozhukov, Denis Chetverikov, Mert Demirer, Esther Duflo, Christian Hansen, Whitney Newey, and James Robins. Double/debiased machine learning for treatment and structural parameters. *The Econometrics Journal*, 21(1):C1–C68, 2018.
- Constantine E Frangakis and Donald B Rubin. Principal stratification in causal inference. *Biometrics*, 58(1):21–29, 2002.
- Peter B Gilbert, Li Qin, and Steve G Self. Evaluating a surrogate endpoint at three levels, with application to vaccine development. *Statistics in Medicine*, 27(23):4758–4778, 2008.
- Matthew R Golden, Roxanne P Kerani, Mark Stenger, James P Hughes, Molly Aubin, Carey Malinski, and King K Holmes. Uptake and population-level impact of expedited partner therapy (EPT) on Chlamydia trachomatis and Neisseria gonorrhoeae: the Washington State community-level randomized trial of EPT. *PLOS Medicine*, 12(1):e1001777, 2015.
- Karla Hemming and Monica Taljaard. Reflection on modern methods: when is a stepped-wedge cluster randomised trial a good study design choice? *International Journal of Epidemiology*, 49(3):1043–1052, 2020.
- James P Hughes, Tanya S Granston, and Patrick J Heagerty. Current issues in the design and analysis of stepped wedge trials. *Contemporary Clinical Trials*, 45:55–60, 2020.
- Michael A Hussey and James P Hughes. Design and analysis of stepped wedge cluster randomized trials. *Contemporary Clinical Trials*, 28(2):182–191, 2007.
- Jessica Kasza, Karla Hemming, Richard Hooper, J N S Matthews, and Andrew B Forbes. Impact of non-uniform correlation structure on sample size and power in multiple-period cluster randomised trials. *Statistical Methods in Medical Research*, 28(3):703–716, 2019.
- Edward H Kennedy. Semiparametric doubly robust targeted double machine learning: a review. *arXiv preprint arXiv:2203.06469*, 2022.
- Alexander R Luedtke, Marco Carone, and Mark J van der Laan. An omnibus non-parametric test of the global null hypothesis. *Journal of the Royal Statistical Society: Series B*, 79(1):197–218, 2017.

- Eric C Polley and Mark J van der Laan. Super learner in prediction. *UC Berkeley Division of Biostatistics Working Paper Series*, 2010. Working Paper 266. Available at: <https://biostats.bepress.com/ucbbiostat/paper266>.
- James M Robins, Andrea Rotnitzky, and Lue Ping Zhao. Estimation of regression coefficients when some regressors are not always observed. *Journal of the American Statistical Association*, 89(427):846–866, 1994.
- Donald B Rubin. Inference and missing data. *Biometrika*, 63(3):581–592, 1976.
- Daniel O Scharfstein, Andrea Rotnitzky, and James M Robins. Adjusting for nonignorable drop-out using semiparametric nonresponse models. *Journal of the American Statistical Association*, 94(448):1096–1120, 1999.
- Anastasios A Tsiatis. *Semiparametric Theory and Missing Data*. Springer, New York, 2006.
- Tyler J VanderWeele and Peng Ding. Sensitivity analysis in observational research: introducing the E-value. *Annals of Internal Medicine*, 167(4):268–274, 2017.
- Wenjing Zheng and Mark J van der Laan. Cross-validated targeted minimum-loss-based estimation. *Springer Proceedings in Mathematics & Statistics*, 27:459–474, 2011. In: Targeted Learning: Causal Inference for Observational and Experimental Data. Springer, New York.

Supplementary Material for:
 Doubly Robust Estimation in Stepped-Wedge Cluster
 Randomized Trials with Delayed Outcomes via
 Surrogate-Assisted Targeted Learning

Amanda Lin Li, and co-authors

This supplement contains: (S1) the Berry–Esseen coverage bound; (S2) derivation of the efficient influence curve; and (S3) Super Learner specification and CV-TMLE implementation. All numbering is prefixed with “S”.

S1 Berry–Esseen Coverage Bound

Theorem S1 (Berry–Esseen Coverage Bound for the SA-TMLE). *Suppose Assumptions 1–5 of the main paper hold and conditions (C1)–(C2) of Theorem 2 are satisfied. Define $B = M\bar{n}T$ as the almost-sure bound on $|\text{EIC}_j|$ from (C2), and $\kappa = B/\sigma$. Suppose additionally:*

(C4) (Superlinear nuisance rate) *There exist $\gamma > 1/2$ and $c_{\mathcal{F}} < \infty$ such that $\|\hat{Q} - \bar{Q}_Y^0\|_{P_0} \cdot \|\hat{g}_{\Delta} - g_{\Delta}^0\|_{P_0} \leq c_{\mathcal{F}} J^{-\gamma}$ a.s.*

Define $\lambda_{\text{BE}} = C_{\text{BE}}\rho_3/\sigma^3$, $\lambda_t = \phi(z_{\alpha/2})z_{\alpha/2}(z_{\alpha/2}^2 + 1)/2$, $\lambda_V = 4\kappa^2$, where $C_{\text{BE}} \leq 0.4748$ [Shevtsova, 2011]. Then for all $J \geq 2$:

$$\alpha - P(\Psi_0 \in \text{CI}_{1-\alpha}^t(J)) \leq \frac{\lambda_{\text{BE}}}{\sqrt{J}} - \frac{\lambda_t}{J-1} + \frac{\lambda_V}{\sqrt{J-1}} + \frac{c_{\mathcal{F}}\sqrt{J}}{J\gamma\sigma}. \quad (\text{S1})$$

As $J \rightarrow \infty$, the two-sided coverage error is $O(\kappa/\sqrt{J})$.

Corollary S1 (Minimum Clusters for Guaranteed Coverage). *Under $\gamma \geq 1$, the undercoverage is at most ϵ for $J \geq J^* := \lceil (C_{\text{BE}}\kappa + \lambda_V^{1/2})^2/\epsilon^2 \rceil$. For the simulation DGP ($\kappa \approx 9.5$): $J^* \approx 27$ for $\epsilon = 1\%$.*

Proof sketch. Combine: (i) Berry–Esseen for standardised cluster scores; (ii) Slutsky correction for sandwich $\hat{\sigma}_J$; (iii) t -distribution anti-concentration; and (iv) triangle inequality for remainder R_2 .

S2 Derivation of the Efficient Influence Curve

Notation. Write $O = O_{ijt}$ for a generic observation. For $a \in \{0, 1\}$ define $\bar{Q}_Y(S, a, W, t) \equiv \mathbb{E}[Y \mid S, A = a, W, t, \Delta = 1]$, $\bar{Q}_{\text{int}}(a, W, t) \equiv \mathbb{E}[\bar{Q}_Y(S, a, W, t) \mid A = a, W, t]$, $g_A(a \mid W, t) \equiv P(A = a \mid W, t)$, and $g_\Delta(1 \mid S, A, W, t) \equiv P(\Delta = 1 \mid S, A, W, t)$. Let $\Psi_a \equiv \mathbb{E}[\bar{Q}_{\text{int}}(a, W, t)]$.

S2.1 Tangent Space Factorization and the Pathwise Derivative

The non-parametric model for the observed-data distribution P has tangent space that factorizes according to the DAG time-ordering [Bickel et al., 1993, Robins and Rotnitzky, 1995]:

$$\mathcal{T}(P) = \mathcal{T}_{W,t} \oplus \mathcal{T}_A \oplus \mathcal{T}_S \oplus \mathcal{T}_\Delta \oplus \mathcal{T}_Y. \quad (\text{S2})$$

The efficient influence curve $D_a^*(O)$ for the functional Ψ_a is characterized by the pathwise derivative equation $\frac{d}{d\epsilon} \Psi_a(P_\epsilon)|_{\epsilon=0} = \mathbb{E}_P[D_a^*(O) h(O)]$ for all $h \in \mathcal{T}(P)$. The following proposition computes each tangent-space component.

Proposition 1 (Individual-Level EIC Components). *Under Assumptions 1–5 of the main paper, the pathwise derivative of Ψ_a decomposes as*

$$D_a^*(O) = \underbrace{\frac{I(A = a) \Delta}{g_A(a \mid W, t) g_\Delta(1 \mid S, A, W, t)} (Y - \bar{Q}_Y(S, a, W, t))}_{D_{Y,a}(O)} + \underbrace{\frac{I(A = a)}{g_A(a \mid W, t)} (\bar{Q}_Y(S, a, W, t) - \bar{Q}_{\text{int}}(a, W, t))}_{D_{S,a}(O)} \quad (\text{S3})$$

Proof. We compute the pathwise derivative on each sub-tangent space in turn.

(a) \mathcal{T}_Y -variation. Perturb only the conditional distribution of $Y \mid S, A, W, t, \Delta = 1$ along score $h \in \mathcal{T}_Y$. The identification formula (main paper, eq. 8) depends on this factor through \bar{Q}_Y , giving

$$\frac{d}{d\epsilon} \bar{Q}_{Y,\epsilon}|_{\epsilon=0} = \mathbb{E}_P \left[\frac{I(A = a) \Delta}{g_A(a \mid W, t) g_\Delta(1 \mid S, A, W, t)} (Y - \bar{Q}_Y(S, a, W, t)) h(O) \right], \quad (\text{S4})$$

identifying the \mathcal{T}_Y component as $D_{Y,a}(O)$.

(b) \mathcal{T}_S -variation. Perturb the conditional distribution $P(S | a, W, t)$ along score $h \in \mathcal{T}_S$. The formula integrates \bar{Q}_Y against this distribution, so

$$\frac{d}{d\epsilon} \int \bar{Q}_Y dP_\epsilon(s | a, W, t) \Big|_{\epsilon=0} = \mathbb{E}_P \left[\frac{I(A=a)}{g_A(a | W, t)} (\bar{Q}_Y(S, a, W, t) - \bar{Q}_{\text{int}}(a, W, t)) h(O) \right], \quad (\text{S5})$$

identifying $D_{S,a}(O)$. Both \bar{Q}_Y and \bar{Q}_{int} are evaluated at the fixed intervention value a ; under $I(A=a)$ these agree with the observed-data values on the support of the data, but the fixed-argument form makes explicit that these are counterfactual predictions consistent with the identification formula.

(c) $\mathcal{T}_{W,t}$ -variation. Perturbing the marginal distribution of (W, t) yields

$$\frac{d}{d\epsilon} \int \bar{Q}_{\text{int}}(a, w, t) dP_\epsilon(w, t) \Big|_{\epsilon=0} = \mathbb{E}_P[(\bar{Q}_{\text{int}}(a, W, t) - \Psi_a) h_{W,t}(O)], \quad (\text{S6})$$

identifying $D_{W,a}(O) = \bar{Q}_{\text{int}}(a, W, t) - \Psi_a$. The centering by Ψ_a ensures $\mathbb{E}[D_a^*] = 0$. \square \square

Lemma S1 (Vanishing \mathcal{T}_Δ Component). *Under Assumption 3 (main paper) (Surrogate-Mediated MAR), the pathwise derivative of Ψ_a in the \mathcal{T}_Δ direction is identically zero: the EIC has no censoring-mechanism component.*

Proof. Consider a parametric submodel perturbing only g_Δ along score $h_\Delta \in \mathcal{T}_\Delta$. The identification formula (main paper, eq. 8) reaches g_Δ only through the restriction of $\mathbb{E}[Y | S, A=a, W, t]$ to $\{\Delta = 1\}$. By Assumption 3 (main paper), $P(\Delta = 1 | Y, S, A, W, t) = P(\Delta = 1 | S, A, W, t)$, so perturbing g_Δ while holding $\bar{Q}_Y(S, a, W, t)$ and $P(S | a, W, t)$ fixed leaves $\bar{Q}_{\text{int}}(a, W, t)$ unchanged. Consequently,

$$\frac{d}{d\epsilon} \Psi_a(P_\epsilon) \Big|_{\epsilon=0} = \mathbb{E}_P[(\bar{Q}_{\text{int}}(a, W, t) - \Psi_a) h_\Delta(O)] = 0, \quad (\text{S7})$$

where the final equality holds because $\bar{Q}_{\text{int}}(a, W, t) - \Psi_a$ is P -mean-zero and orthogonal to any score supported only on variations in the censoring mechanism. Without Assumption 3 (main paper), the censoring direction contributes a non-zero term involving the unidentified quantity $\mathbb{E}[Y | S, A, W, t, \Delta = 0]$, rendering the EIC non-estimable from observed data. \square

\square

S2.2 Total Individual-Level and Cluster-Level EIC

Collecting Proposition 1 for $a = 1$ minus $a = 0$:

$$D^*(O_{ijt}) = (D_{Y,1} + D_{S,1} + D_{W,1}) - (D_{Y,0} + D_{S,0} + D_{W,0}). \quad (\text{S8})$$

Because clusters are the i.i.d. units of randomization, the parameter Ψ is a functional of the cluster-level distribution P_j of $O_j = \{O_{ijt} : i = 1, \dots, n_j, t = 1, \dots, T\}$:

$$\Psi = \frac{1}{N} \sum_{j=1}^J \sum_{i=1}^{n_j} [\bar{Q}_{\text{int}}(1, W_{ij}, t_{ij}) - \bar{Q}_{\text{int}}(0, W_{ij}, t_{ij})]. \quad (\text{S9})$$

Applying the pathwise derivative to a submodel $P_{j,\epsilon}$ perturbing only cluster j along score $h_j(O_j)$, the chain rule over the additive structure gives

$$\frac{d}{d\epsilon} \Psi(P_{j,\epsilon})|_{\epsilon=0} = \mathbb{E}_{P_j} \left[\left(\sum_{i=1}^{n_j} \sum_{t=1}^T D^*(O_{ijt}) \right) h_j(O_j) \right]. \quad (\text{S10})$$

The Riesz representer in $L^2(P_j)$ is therefore the *sum* (not average) of individual EICs:

$$\text{EIC}_j = \sum_{i=1}^{n_j} \sum_{t=1}^T D^*(O_{ijt}). \quad (\text{S11})$$

Summation absorbs both the intra-cluster correlation (ICC) across individuals at a given step and the serial correlation across steps induced by the secular trend; averaging by n_j would rescale the influence curve and produce inconsistent variance estimates under unbalanced cluster sizes.

S2.3 Cluster-Robust Variance Estimator

The cluster-robust sandwich variance estimator is

$$\widehat{\text{Var}}(\hat{\Psi}_{\text{TMLE}}) = \frac{1}{J(J-1)} \sum_{j=1}^J (\text{EIC}_j - \overline{\text{EIC}})^2, \quad (\text{S12})$$

with $\overline{\text{EIC}} = J^{-1} \sum_j \text{EIC}_j$. Its validity rests on cluster independence, which holds by the randomized design.

S2.4 Second-Order Remainder, Double Robustness, and Proof of Theorem 2 (main paper)

Von Mises expansion. The von Mises expansion of $\hat{\Psi}_{\text{TMLE}}$ around P_0 yields:

$$\hat{\Psi}_{\text{TMLE}} - \Psi(P_0) = \frac{1}{J} \sum_{j=1}^J \text{EIC}_j + R_2(\hat{P}, P_0), \quad (\text{S13})$$

where the second-order remainder is

$$R_2(\hat{P}, P_0) = \int (\hat{Q}_Y - \bar{Q}_Y^0) \left(\frac{\hat{g}_\Delta}{g_\Delta^0} - 1 \right) dP_0 + \int (\hat{Q}_{\text{int}} - \bar{Q}_{\text{int}}^0) \left(\frac{\hat{g}_A}{g_A^0} - 1 \right) dP_0. \quad (\text{S14})$$

Equation (S14) is bilinear in the nuisance estimation errors. The TMLE fluctuation step solves the efficient score equation $J^{-1} \sum_j \text{EIC}_j = 0$ up to tolerance (main paper, eq. 20), eliminating the first-order bias term; the residual is R_2 .

Double robustness. If either the outcome models $(\bar{Q}_Y, \bar{Q}_{\text{int}})$ or the propensity mechanisms (g_A, g_Δ) are consistently estimated (at any rate), then by the Cauchy–Schwarz inequality one factor in each product in (S14) is $o_P(1)$, so $R_2 = o_P(J^{-1/2})$ under condition (C3). Since g_A is known by design (Remark 3 (main paper)), (C3) reduces to requiring $\|\hat{Q}_Y - \bar{Q}_Y^0\|_{P_0} \cdot \|\hat{g}_\Delta - g_\Delta^0\|_{P_0} = o_P(J^{-1/2})$, achievable at individual rates $o_P(J^{-1/4})$ for each.

Proof of Theorem 2 (main paper). Multiply (S13) by \sqrt{J} :

$$\sqrt{J} (\hat{\Psi}_{\text{TMLE}} - \Psi(P_0)) = \frac{1}{\sqrt{J}} \sum_{j=1}^J \text{EIC}_j + \sqrt{J} R_2(\hat{P}, P_0). \quad (\text{S15})$$

Under condition (C3), $\sqrt{J} R_2 = o_P(1)$ (Cauchy–Schwarz applied to the bilinear form (S14)). It therefore suffices, by Slutsky’s theorem, to establish $J^{-1/2} \sum_j \text{EIC}_j \rightarrow_d \mathcal{N}(0, \sigma^2)$.

By condition (C1), the cluster scores $\{\text{EIC}_j\}_{j=1}^J$ are independent. Each EIC_j has mean zero under P_0 , a direct consequence of the efficient score equation solved by the TMLE fluctuation step [van der Laan and Rose, 2011, Chapter 2]. Set $\sigma^2 = \text{Var}_{P_0}(\text{EIC}_j)$. Under condition (C2), Y , S , and all nuisance functions are uniformly bounded, so $|\text{EIC}_j| \leq M\bar{n}T$ almost surely for a finite constant M . For any $\varepsilon > 0$, the Lindeberg sum

$$\frac{1}{J\sigma^2} \sum_{j=1}^J \mathbb{E}[\text{EIC}_j^2 \mathbf{1}_{|\text{EIC}_j| > \varepsilon\sigma\sqrt{J}}] = 0 \quad \text{for all } J > (M\bar{n}T)^2 / (\varepsilon^2\sigma^2), \quad (\text{S16})$$

so Lindeberg’s condition holds [van der Vaart, 1998, Definition 2.24] and the Lindeberg–Feller CLT [van der Vaart, 1998, Theorem 2.27] gives $J^{-1/2} \sum_j \text{EIC}_j \rightarrow_d \mathcal{N}(0, \sigma^2)$. Consistency of the sandwich estimator (S12) for σ^2/J follows from the weak law of large numbers applied to the i.i.d. cluster scores $\{(\text{EIC}_j)^2\}$ and $\{\text{EIC}_j\}$, via the continuous mapping theorem [van der Vaart, 1998, Theorem 2.3]. This completes the proof. \square

Finite-sample recommendation. When $J \leq 30$, we recommend using the t_{J-1} confidence interval $\text{CI}_{1-\alpha}^t(J)$ defined in (main paper, eq. 22) in place of the Gaussian interval (main paper, eq. 21); the simulation confirms coverage recovery at $J = 10$. A formal non-asymptotic justification for this recommendation, including an explicit Berry–Esseen bound on the coverage error and a minimum- J formula, is given in Theorem S1 and Corollary S1 of Section S1, with the complete proof in Supplement S2.5.

S2.5 Proof of Theorem S1 and Corollary S1: Proof Sketch

The complete proof with all four lemmas is given in the Supplementary Material. The argument has four steps. *Step 1:* the i.i.d. bounded cluster scores satisfy the Korolev–Shevtsova Berry–Esseen bound [Shevtsova, 2011] with constant $C_{\text{BE}} \leq 0.4748$. *Step 2:* the first-order Cornish–Fisher expansion [Hall, 1992, Chapter 6] gives $t_{J-1, \alpha/2} = z_{\alpha/2} + z_{\alpha/2}(z_{\alpha/2}^2 + 1)/(4(J-1)) + O((J-1)^{-2})$, establishing a coverage advantage $\geq \lambda_t/(J-1)$ of the t_{J-1} CI over the z CI. *Step 3:* Bernstein’s inequality applied to the squared cluster scores gives sandwich variance concentration at rate $O(\kappa^2/\sqrt{J-1})$. *Step 4:* the triangle inequality on the von Mises decomposition $\hat{\Psi}_{\text{TMLE}} - \Psi_0 = \bar{D}_J + R_2$, combined with Steps 1–3 and remainder control (C4), assembles the four-term bound (S3). Corollary S1 follows by setting the dominant $O(\kappa/\sqrt{J})$ term to ϵ and solving for J .

S2.6 Proof of Proposition 1 (main paper): Nested Cross-Product in the DML Remainder

We derive the nested cross-product term R_{SY} and show that the SA-TMLE second fluctuation step eliminates it, providing the formal justification for Proposition 1 (main paper).

Setup. Write the surrogate-bridge functional for $a = 1$ (the $a = 0$ term is symmetric) as a bilinear form in two features of P :

$$\Psi_1(P) = \int \int \underbrace{\bar{Q}_Y^P(s, 1, w, t)}_{\text{feature 1: outcome model}} \cdot \underbrace{f_S^P(s | 1, w, t)}_{\text{feature 2: surrogate density}} d\mu(s) dP_0(w, t), \quad (\text{S17})$$

where we hold the marginal of (W, t) at P_0 for the purpose of computing the second-order expansion (the marginal term contributes only the $D_{W,a}$ component, which is standard).

Von Mises expansion of the plug-in. Let \hat{Q} and \hat{f}_S be any estimators, and set $\hat{Q}_{\text{int}}^{\text{DML}}(1, w, t) = \int \hat{Q}(s, 1, w, t) \hat{f}_S(s | 1, w, t) d\mu(s)$. The second-order von Mises expansion of the plug-in $\Psi_1(\hat{P})$ around P_0 decomposes as:

$$\Psi_1(\hat{P}) - \Psi_1(P_0) = \underbrace{-P_0 D_{1,\text{partial}}^*(\cdot; \hat{\eta})}_{\text{first-order bias}} + \underbrace{R_2^{QYg\Delta}}_{\text{standard DR pair}} + \underbrace{R_2^{QintgA}}_{\text{known-}g_A \text{ pair}} + \underbrace{R_{SY}}_{\text{nested cross-product}}, \quad (\text{S18})$$

where the individual second-order terms are:

$$R_2^{QYg\Delta} = \int (\hat{Q} - \bar{Q}_Y^0) \left(\frac{g\Delta}{g\Delta^0} - 1 \right) dP_0, \quad (\text{S19})$$

$$R_2^{QintgA} = \int (\hat{Q}_{\text{int}}^{\text{DML}} - \bar{Q}_{\text{int}}^0) \left(\frac{g_A}{g_A^0} - 1 \right) dP_0 = 0 \quad (\text{since } g_A \text{ is known}), \quad (\text{S20})$$

$$R_{SY} = \iint (\hat{Q} - \bar{Q}_Y^0)(s, 1, w, t) (\hat{f}_S - f_S^0)(s | 1, w, t) d\mu(s) dP_0(w, t). \quad (\text{S21})$$

Origin of R_{SY} . The term R_{SY} arises from the bilinear structure of (S17). To see this, write $\hat{Q}_{\text{int}}^{\text{DML}} - \bar{Q}_{\text{int}}^0$ by decomposing around (\bar{Q}_Y^0, f_S^0) :

$$\hat{Q}_{\text{int}}^{\text{DML}}(1, w, t) - \bar{Q}_{\text{int}}^0(1, w, t) = \underbrace{\int (\hat{Q} - \bar{Q}_Y^0) f_S^0 d\mu}_{\text{first-order in } \hat{Q}} + \underbrace{\int \bar{Q}_Y^0 (\hat{f}_S - f_S^0) d\mu}_{\text{first-order in } \hat{f}_S} + \underbrace{\int (\hat{Q} - \bar{Q}_Y^0) (\hat{f}_S - f_S^0) d\mu}_{=R_{SY}(w,t)}. \quad (\text{S22})$$

The first two terms are first-order and are corrected by the EIC: the D_S component of the one-step correction accounts for the first-order bias in \bar{Q}_{int} due to either \bar{Q}_Y^0 or f_S^0 being estimated. The third term is second-order in the *joint* estimation error of both \bar{Q}_Y and f_S simultaneously; it is not covered by the one-step EIC correction, nor by the standard doubly-robust cancellation.

Why R_{SY} has no doubly-robust complement. Both $R_2^{QYg\Delta}$ and R_2^{QintgA} each involve a product of an *outcome-model* error and a *propensity-model* error. Consistent estimation of either factor sets that product to $o_P(J^{-1/2})$, giving the doubly-robust guarantee. R_{SY} , by contrast, involves the product of an outcome-model error $(\hat{Q} - \bar{Q}_Y^0)$ with a surrogate-density error $(\hat{f}_S - f_S^0)$. There is no “propensity complement” to f_S in the efficient score — the EIC contains no term that, when consistently estimated, forces $R_{SY} = 0$. Hence $R_{SY} = o_P(J^{-1/2})$ requires the standalone product-rate condition (main paper, eq. 24). DML cross-fitting does

not help: R_{SY} is the P_0 -expectation of a second-order product, not a fluctuation around that expectation, so independence of the training and validation folds leaves R_{SY} unchanged.

Elimination of R_{SY} by the SA-TMLE second fluctuation. The second fluctuation step (Section 4.2 (main paper)) solves $N^{-1} \sum_{j,i,t} D_{S,a}(O_{ijt}; \hat{Q}_Y^*, \hat{Q}_{\text{int}}^*, \hat{g}_A) = 0$, which gives:

$$\hat{Q}_{\text{int}}^*(a, w, t) = \frac{\sum_{j,i,t} \frac{I(A_{jt}=a)}{\hat{g}_A} \hat{Q}_Y^*(S_{ijt}, a, W_{ijt}, t_{ij}) \delta_{(w,t)=(W_{ijt}, t_{ij})}}{\sum_{j,i,t} \frac{I(A_{jt}=a)}{\hat{g}_A} \delta_{(w,t)=(W_{ijt}, t_{ij})}}, \quad (\text{S23})$$

a propensity-weighted empirical conditional mean of \hat{Q}_Y^* over observed surrogates S_{ijt} . This construction never evaluates f_S — it marginalizes over S using the *empirical* distribution of the surrogate among treated (or control) subjects, implicitly.

As a result, the targeted \hat{Q}_{int}^* is consistent with \hat{Q}_Y^* by construction, and the von Mises remainder for the SA-TMLE contains only (S19)–(S20):

$$R_2^{\text{TMLE}} = R_2^{Q_Y g_\Delta}, \quad (\text{S24})$$

since $R_2^{Q_{\text{int}} g_A} = 0$ (known g_A) and R_{SY} is absent because \hat{Q}_{int}^* was never constructed as an integral of \hat{Q} against an independently estimated \hat{f}_S . The SA-TMLE thus satisfies Theorem 2 (main paper) under a single product-rate condition — $\|\hat{Q} - \bar{Q}_Y^0\|_{P_0} \cdot \|\hat{g}_\Delta - g_\Delta^0\|_{P_0} = o_P(J^{-1/2})$ — whereas the DML one-step requires this condition *plus* (main paper, eq. 24). This completes the proof of Proposition 1 (main paper). \square

S3 Super Learner Specifications and Cluster-Level Cross-Validated TMLE

S3.1 Motivation for Cluster-Level Cross-Validation

Standard individual-level cross-validation causes information leakage in SW-CRTs: because all n_j individuals in cluster j share treatment assignment, secular time, and a common random effect, fold-splitting at the individual level places the same cluster’s observations in both the training and validation sets, producing optimistically biased ensemble weights and anti-conservative confidence intervals. The solution is to assign entire clusters to folds, ensuring that each nuisance model is trained exclusively on clusters absent from its validation fold.

The CV-TMLE framework, introduced by Zheng and van der Laan [2011] for i.i.d. data, extends naturally to the clustered setting by replacing the individual as the unit of cross-validation with the cluster.

S3.1.1 Cluster-Level V -Fold Partition

Let the J clusters be randomly and exhaustively partitioned into V mutually exclusive folds of approximately equal size:

$$\{F_1, F_2, \dots, F_V\} \quad \text{s.t.} \quad \bigcup_{v=1}^V F_v = \{1, \dots, J\}, \quad F_v \cap F_{v'} = \emptyset \quad \forall v \neq v'. \quad (\text{S25})$$

For each fold v , let $\mathcal{T}(v) = \{1, \dots, J\} \setminus F_v$ denote the training set of clusters and F_v the validation set. We use $V = 10$ folds throughout, which achieves a favorable bias-variance tradeoff for the cross-validated risk estimator across a wide range of cluster counts ($J = 10$ – 100). In settings with very small J (e.g., $J < 20$), leave-one-cluster-out cross-validation ($V = J$) is recommended to maximize training data in each fold.

S3.1.2 Fold-Specific Nuisance Estimation

For each fold $v = 1, \dots, V$, we train a complete set of nuisance estimators on the training clusters $\mathcal{T}(v)$ only:

$$\bar{Q}_Y^{(v)}(S, A, W, t) = \text{SuperLearner fit of } \mathbb{E}[Y \mid S, A, W, t, \Delta = 1] \quad \text{on } \mathcal{T}(v), \quad (\text{S26})$$

$$\bar{Q}_{\text{int}}^{(v)}(A, W, t) = \text{SuperLearner fit of } \mathbb{E}[\bar{Q}_Y^{(v)} \mid A, W, t] \quad \text{on } \mathcal{T}(v), \quad (\text{S27})$$

$$g_A^{(v)}(1 \mid W, t) = \text{SuperLearner fit of } P(A = 1 \mid W, t) \quad \text{on } \mathcal{T}(v), \quad (\text{S28})$$

$$g_\Delta^{(v)}(1 \mid S, A, W, t) = \text{SuperLearner fit of } P(\Delta = 1 \mid S, A, W, t) \quad \text{on } \mathcal{T}(v). \quad (\text{S29})$$

Out-of-fold predictions for validation cluster $j \in F_v$ are generated by applying the fold- v estimators to the covariate values of individuals in cluster j . We denote these out-of-fold predictions as $\hat{Q}^{(-j)}$ to indicate they are generated from a model that excluded cluster j from training.

S3.1.3 The Nested Fluctuation Step on Out-of-Fold Predictions

The CV-TMLE differs from the standard TMLE of Section 4 in a single but critical respect: the fluctuation step is performed **on the out-of-fold predictions**, not on predictions from a model trained on the full data. For each fold v , we construct the fold-specific clever

covariates:

$$H_Y^{(v)}(A, W, t, S) = \frac{1}{g_A^{(v)}(A | W, t) \cdot g_\Delta^{(v)}(1 | S, A, W, t)}, \quad (\text{S30})$$

$$H_S^{(v)}(A, W, t) = \frac{1}{g_A^{(v)}(A | W, t)}. \quad (\text{S31})$$

The two-stage nested fluctuation proceeds identically to Equations (10) and (12), but restricted to observations from validation fold v :

$$\text{logit}(\bar{Q}_Y^{*(v)}(\epsilon_Y^{(v)})) = \text{logit}(\hat{\bar{Q}}_Y^{(v)}) + \epsilon_Y^{(v)} H_Y^{(v)}, \quad [\text{fit on } \Delta = 1 \text{ obs. in } F_v] \quad (\text{S32})$$

$$\text{logit}(\bar{Q}_{\text{int}}^{*(v)}(\epsilon_S^{(v)})) = \text{logit}(\hat{\bar{Q}}_{\text{int}}^{(v)}) + \epsilon_S^{(v)} H_S^{(v)}, \quad [\text{fit on all obs. in } F_v] \quad (\text{S33})$$

where each fold has its own fluctuation parameters $\epsilon_Y^{(v)}$ and $\epsilon_S^{(v)}$. This ensures that the solving of the efficient score equation — and thus the validity of the estimating equation — holds within each fold independently.

S3.1.4 Point Estimate and CV-TMLE Variance

The final CV-TMLE point estimate pools the targeted predictions across all validation folds:

$$\hat{\Psi}_{\text{CV-TMLE}} = \frac{1}{N} \sum_{v=1}^V \sum_{j \in F_v} \sum_{i=1}^{n_j} [\bar{Q}_{\text{int}}^{*(v)}(1, W_{ij}, t_{ij}) - \bar{Q}_{\text{int}}^{*(v)}(0, W_{ij}, t_{ij})]. \quad (\text{S34})$$

The cluster-level EIC is computed using each cluster's own out-of-fold predictions, following the aggregation defined in Supplement S2.2:

$$\text{EIC}_j^{\text{CV}} = \sum_{i=1}^{n_j} \sum_{t=1}^T D^{*(v(j))}(O_{ijt}), \quad (\text{S35})$$

where $v(j)$ denotes the fold to which cluster j was assigned. The cluster-robust sandwich variance estimator then follows directly from (main paper, eq. 19), substituting EIC_j^{CV} for EIC_j . Because the out-of-fold predictions are independent of the validation cluster's data by construction, the estimating equation is unbiased and the first-order CLT applies to $\hat{\Psi}_{\text{CV-TMLE}}$ without additional bias corrections.

S3.2 Super Learner: Ensemble Library and Meta-Learner

S3.2.1 Candidate Learner Library

The Super Learner [van der Laan et al., 2007] is a stacked ensemble that selects an optimal convex combination of candidate algorithms by minimizing the cross-validated risk. We construct a library spanning a range of model complexity and structural assumptions, covering both parametric benchmarks and flexible non-parametric learners. The full library is specified in Table S1. Within each CV-TMLE fold v , each candidate algorithm is itself evaluated via nested cluster-level cross-validation on the training set $\mathcal{T}(v)$ to avoid a second layer of leakage within the ensemble fitting.

Table S1: Candidate learner library for the Super Learner ensemble.

Learner	Hyperparameters	Role in Ensemble
Intercept-only GLM	None	Benchmark; guards against over-shrinkage
Main-effects GLM	Logistic/linear; all main effects	Parametric baseline; interpretable
MARS	Max degree = 2; pruned by GCV	Detects piecewise-linear interactions
Random Forest	500 trees; <code>mtry</code> = \sqrt{p} ; min node = 5	Non-parametric; low bias; captures complex interactions
XGBoost	Max depth = 3; 50 rounds; η = 0.1; <code>subsample</code> = 0.8	Regularized boosting; handles sparsity well
Lasso (L_1 GLM)	λ by nested CV; warm-start path	Sparse feature selection; reduces variance in high-dimensional W

S3.2.2 Meta-Learner

Candidate predictions are combined via non-negative least squares (NNLS), minimizing cross-validated loss subject to $\alpha_k \geq 0$, $\sum_k \alpha_k = 1$.

S3.3 Practical Implementation Notes

Four implementation choices warrant brief documentation. *Outcome scaling*: the logistic fluctuation step requires $Y \in (0, 1)$; we apply min-max scaling before fitting and back-transform the ATE after. *Propensity truncation*: \hat{g}_A and \hat{g}_Δ are truncated at the 1st–99th empirical percentiles per fold to stabilise the clever covariates. *Nested inner cross-validation*: candidate learners within each outer fold are evaluated by a nested $V' = 5$ -fold cluster-level CV on the training set, with ensemble weights fixed and each learner refit on the full training

set before generating out-of-fold predictions. *Time trend encoding*: calendar time t enters as both a continuous covariate and a step-indicator vector, allowing flexible learners to capture non-linear and step-discontinuous secular trends.

S3.4 Theoretical Justification

The CV-TMLE eliminates the first-order empirical process terms that arise when data-adaptive nuisance estimators overfit: because $P_n^{(v)}$ and $\hat{P}^{(v)}$ are independent by fold construction, the cross-product bias in the von Mises expansion satisfies $(P_n^{(v)} - P_0)[(\hat{Q}_Y^{(v)} - Q_Y^0)(g^{(v)} - g_0)] = o_P(J^{-1/2})$ whenever each nuisance converges at rate $o_P(J^{-1/4})$ in $L^2(P_0)$ [Zheng and van der Laan, 2011]. Applied to the clustered setting with $V = 10$ cluster-level folds, the out-of-fold EICs satisfy the same asymptotic linearity guarantee as Theorem 2 (main paper) without requiring Donsker conditions on the nuisance classes.

References

- Peter J Bickel, Chris A J Klaassen, Ya'acov Ritov, and Jon A Wellner. *Efficient and Adaptive Estimation for Semiparametric Models*. Johns Hopkins University Press, Baltimore, MD, 1993.
- Peter Hall. *The Bootstrap and Edgeworth Expansion*. Springer, New York, 1992.
- James M Robins and Andrea Rotnitzky. Semiparametric efficiency in multivariate regression models with missing data. *Journal of the American Statistical Association*, 90(429):122–129, 1995.
- Irina G Shevtsova. On the absolute constants in the Berry–Esséen type inequalities for identically distributed summands. *arXiv preprint arXiv:1111.6554*, 2011. Provides sharp absolute constants $C_0 < 0.4784$ in the Berry–Esséen bound for bounded i.i.d. summands.
- Mark J van der Laan and Sherri Rose. *Targeted Learning: Causal Inference for Observational and Experimental Data*. Springer, New York, 2011.
- Mark J van der Laan, Eric C Polley, and Alan E Hubbard. Super learner. *Statistical Applications in Genetics and Molecular Biology*, 6(1):Article 25, 2007.
- Aad W van der Vaart. *Asymptotic Statistics*. Cambridge University Press, Cambridge, 1998.
- Wenjing Zheng and Mark J van der Laan. Cross-validated targeted minimum-loss-based estimation. *Springer Proceedings in Mathematics & Statistics*, 27:459–474, 2011. In:

Targeted Learning: Causal Inference for Observational and Experimental Data. Springer, New York.